FLOW STUDY OF THE NOZZLE REGION OF THE SPACE SHUTTLE SOLID ROCKET MOTOR

by

DANIEL E. SQUIRE

Thesis submitted to the Faculty of the
Virginia Polytechnic Institute and State University
in partial fulfillment of the requirements for the degree of

MASTER OF SCIENCE

in

AEROSPACE ENGINEERING

APPROVED:

W. L. Neu

J. F. Marchman III

D. A. Walker

April 1988
Blacksburg, Virginia

ABSTRACT

A flow visualization study was conducted to analyze flow characteristics inside the solid rocket motor (SRM) used on the NASA space shuttle. The objective of this investigation was to determine whether the internal flow structure could adversely affect the nozzle/case joint and the surrounding casing. Also, it was hoped to learn more about causes of low level acoustic pressure oscillations observed during SRM test firings.

The SRM was simulated by water flow through a plexiglas model mounted in a water tunnel. Dye and hydrogen bubble visualization techniques along with hot water analysis methods were used to detect flow patterns. Visual results recorded on video tape indicated strong circumferential and recirculation flows around the nozzle.

Vortex formation near the nozzle inlet was also observed and was the prime focus of this investigation. Because the nozzle inlet geometry was very similar to an aircraft engine inlet operating close to the ground, vortices seen in this investigation were believed to behave like vortices seen around engine inlets. Based on the results from this investigation and the results of previous engine inlet vortex studies, it was concluded that the nozzle vortices could be the excitation source of SRM pressure oscillations.

ACKNOWLEDGEMENTS

This thesis is based on a larger project which involved the cooperative effort of many students and several faculty members. Three teams worked together to accomplish this project. One team led by Dr. D. Walker designed and built the entire water tunnel facility for this investigation. The second team led by Dr. W. Neu constructed the propellant sections of the model. Dr. J. Marchman was the lead coordinator for the project and also led a separate team which designed and built the nozzle section. The time scheduling for completion of the project was ambitious but was successfully met.

The author also wishes to acknowledge Mr. S. Kuppa for his work with hot water thermocouple analysis and data acquisition. In addition the author thanks Mr. S. Ahn and Mr. G. Hsu for their untiring effort in designing and building the water tunnel. Mr. X. Qian provided substantial assistance in constructing the model and data analysis.

The initial part of this project was conducted under a grant from Atlantic Research Corporation in support of Morton Thiokol. Dr. R. Waesche of Atlantic Research Corporation provided technical management as well as assistance in test setup and running. Mr. J. Oliva representing Morton Thiokol also provided technical consulting expertise and assistance

in running tests. Appendix A.1 presents organization of the Solid Rocket Motor (SRM) Flow Study Team as well as a list of participants.

TABLE OF CONTENTS

LIST OF FIGURES

1.0 INTRODUCTION

The space shuttle solid rocket motor (SRM) has been the subject of considerable research. References <1-8> contain a partial listing of recent research projects and analyses. Most of this research has focused on improving the aft field joint. This joint which is necessary because the rocket is partially assembled at the launch site, contains ´0´ rings to prevent leakage of combustion gases. Figure (1) shows a drawing of the SRM and the ´0´ rings. The ´0´ rings are furthered sealed and protected by a special putty. It is thought that during the Challenger accident two or more holes in the putty allowed gas to flow circumferentially around the ´0´ rings resulting in convective heating and their eventual breakdown. However, the rate and cause of the circumferential flow could not be established because the internal flow structure of the SRM was largely unknown. Therefore, the basic purpose of several research projects was to learn more about circumferential flow in the aft joint area.

Because there is a similar ´0 ´ring located in the rear of the SRM (figure (1)), flow patterns in the nozzle section were also of concern. The nozzle is known as a submerged nozzle because its inlet lip extends upstream into the main core flow and can pivot $\pm$ 8 degrees (see figure (2)).

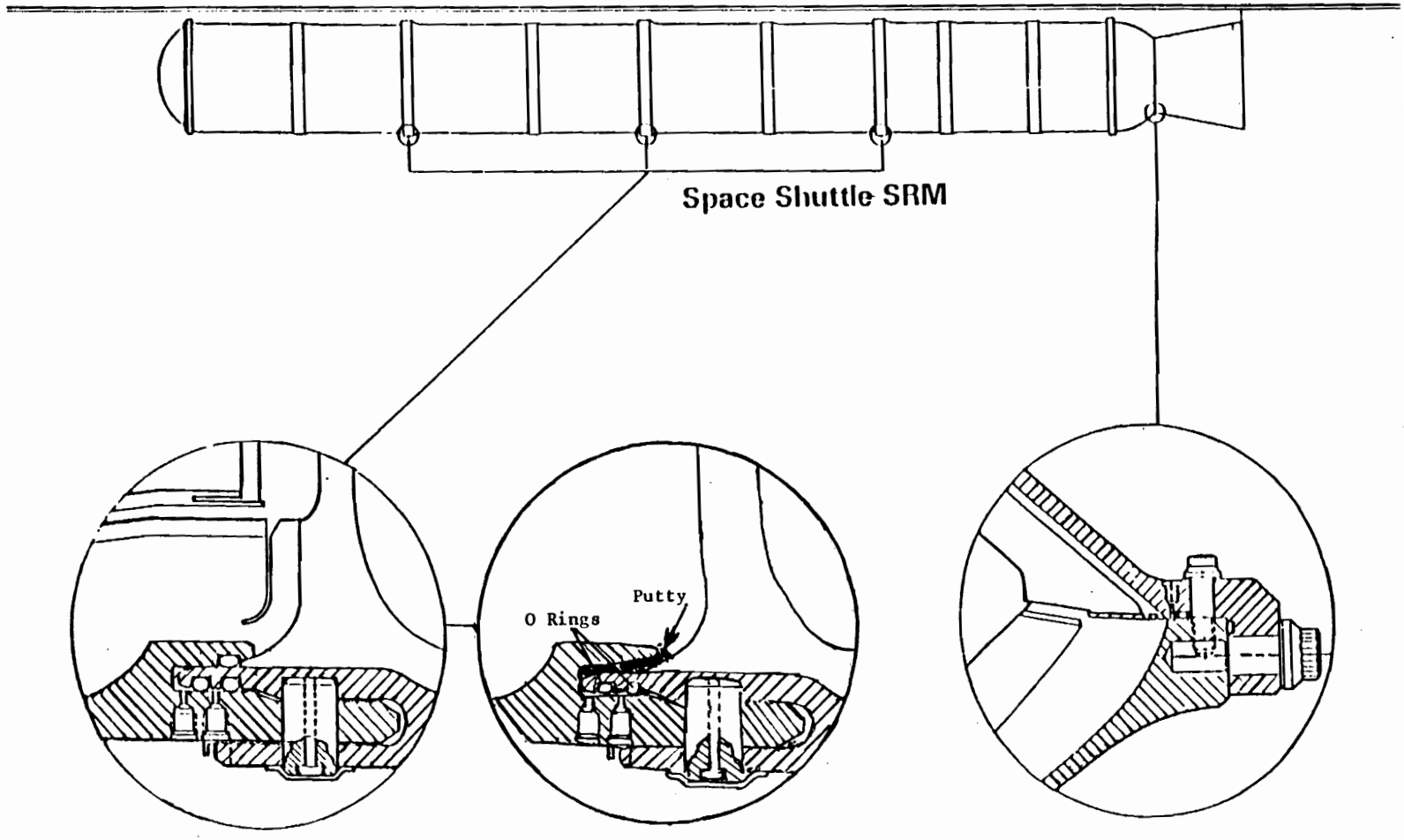

FIELD JOINT (NEW)

FIELD JOINT (OLD)

NOZZLE/CASE JOINT

AFT FIELD JOINT AND NOZZLE/CASE JOINT

Figure 1

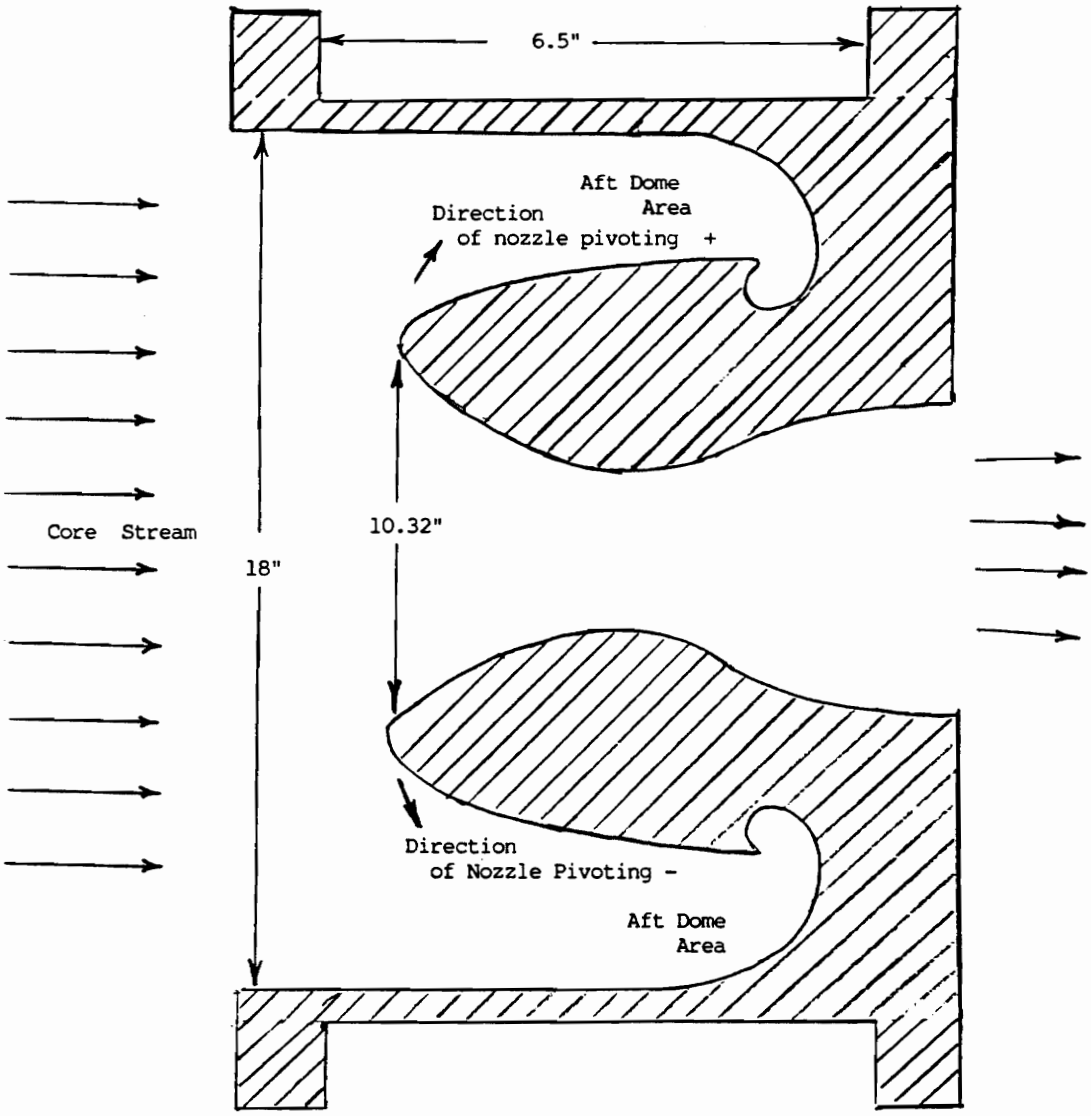

NOZZLE SKETCH

Figure 2

This design is necessary to alter the thrust vector on either of the two SRMs. Nozzle pivoting was certain to cause circumferential flows and was an item of study for several other research projects.

Another flow study objective was to determined the cause of low level pressure oscillations detected during actual SRM firings. These oscillations have been detected at the 15, 30, and 45 Hz ranges and are the first, second and third SRM vibration modes (i.e. 1-L, 2-L and 3-L) respectively <9>. Figure (3) shows the oscillation frequencies detected throughout the burn cycle. Peak to peak pressure displacements were determined based on the mean SRM internal pressure at 80 seconds of burn time. These oscillations are thought to be caused by some type of flow disturbances inside the SRM. In other theories the oscillations have been explained by ring vortices forming from inhibitors <9,10>. The inhibitor is the section at the top of each propellant section which prevents the premature burnback of the propellant (fig (4)). As the propellant burns, the inhibitor burns at a slower rate exposing an edge from which ring vortices can originate. It is thought that vortices formed from the inhibitors do so at the above frequencies and thereby induce oscillations. This thesis will present some contrary evidence that might suggest that vortices forming in

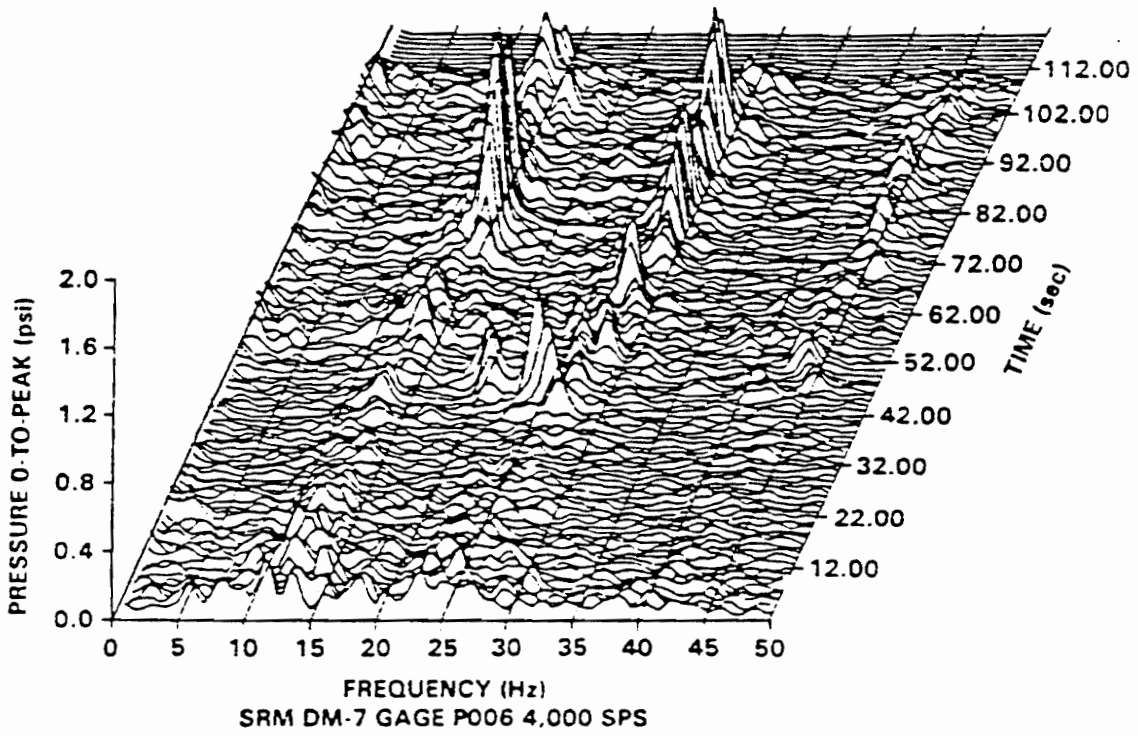

Figure 3. Waterfall Plot of DM-7 Headend Dynamic Pressure

(Reference 9)

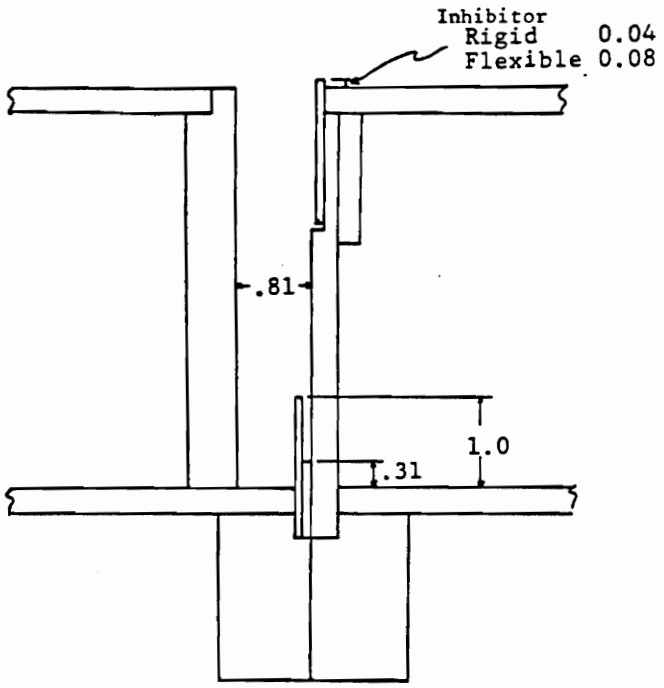

a) 10 sec case

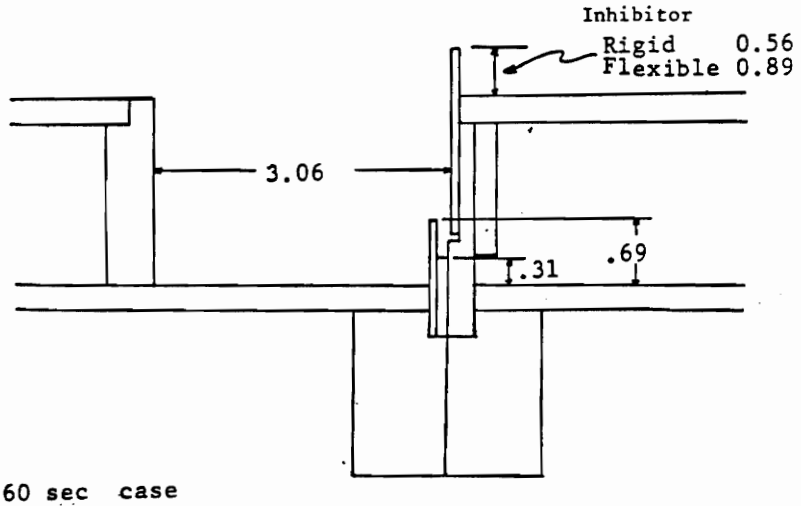

b) 60 sec case

FIGURE 4 MODEL JOINT CONFIGURATION
(All dimensions in inches)

the nozzle region may be the excitation source for SRM acoustic pressure oscillations.

The initial investigation which this thesis is based on was done by Marchman, Neu, Walker et al <8>. This investigation involved cold flow (water tunnel) modeling of the SRM and analysis of all the above mention research objectives. This thesis however will concentrate on the flow phenomena that occurred in the nozzle section. Included in this thesis is the original nozzle study results done during the above mentioned investigation. They are presented here because the author assisted in the investigation and they provide the basis to explain subsequent detailed studies.

All of the investigations were done in a water tunnel because its higher viscosity makes it an excellent medium to model high Reynolds number phenomena at much slower speeds. Water is also excellent for dye visualization.

Previous water tunnel work has shown excellent correlation between combustion model and actual combustion systems. For example, work done by Kennedy <11> showed that water tunnel results could be used to model a rocket ramjet combustor. This study involved flow visualization employing fluorescein dye, neutrally buoyant beads and air bubbles. During this investigation, the Reynolds number based on inlet conditions was between 10^4 and 10^6. The observed results did not vary

and were found to agree with the actual combustor tests.

Schetz et al<12,13,14> also demonstrated the use of cold flow testing with both air and water for improving combustor performance. Studies which investigated the flow field in solid fuel-ramjet combustor where the effects of variations in injector type, and turning vanes were done utilizing a water tunnel. Also a ramjet model where the effect of swirl generated by a swirler installed in an S-turn inlet was investigated. Results from water tunnel work agreed very well with actual combustor results and the water tunnel predictions were used successfully to enhance combustor performance.

Winter et al <15,16,17> also worked with combustion in gas turbine engines which involved understanding swirl, skin cooling, and residence times. All were found to be adequately modeled in the water tunnel.

All of the above work was done with a Reynolds number greater than 10^4. Although these studies did not always match the actual system Reynolds number, good results were obtained. The model SRM Reynolds number, was about 10^5 (based on inlet conditions and diameters) and is believed to be representative of the actual SRM.

2.0 WATER TUNNEL FACILITY

Figure (7) shows the water tunnel. A transparent plexiglas model which simulated two thirds of SRM was mounted in the eight foot test section. The test section was comprised of a steel frame with two glass sides and a bottom. When the test section and water tunnel were filled, water surrounding the model minimized visual distortion and provided essentially an unobstructed view of the model from any angle. To simulate burning propellant approximately half of the flow was diverted from the main tunnel through a plenum section which was connected to the model by several polyurethane tubes. The remaining water tunnel flow passed through the upstream end of the model and simulated the mass flow from SRM propellant sections that were not modeled.

The plenum section was divided into three sections. Each fed a different section of the model. Flow through each plenum section was controlled by a butterfly valve located before the plenum on each of three 5 1/4 inch pipes. The first upstream plenum segment had four hoses which connected to the first upstream section of the model section. This section simulated 20 percent of one full scale booster segment. The second and third plenum segments had 12 hoses

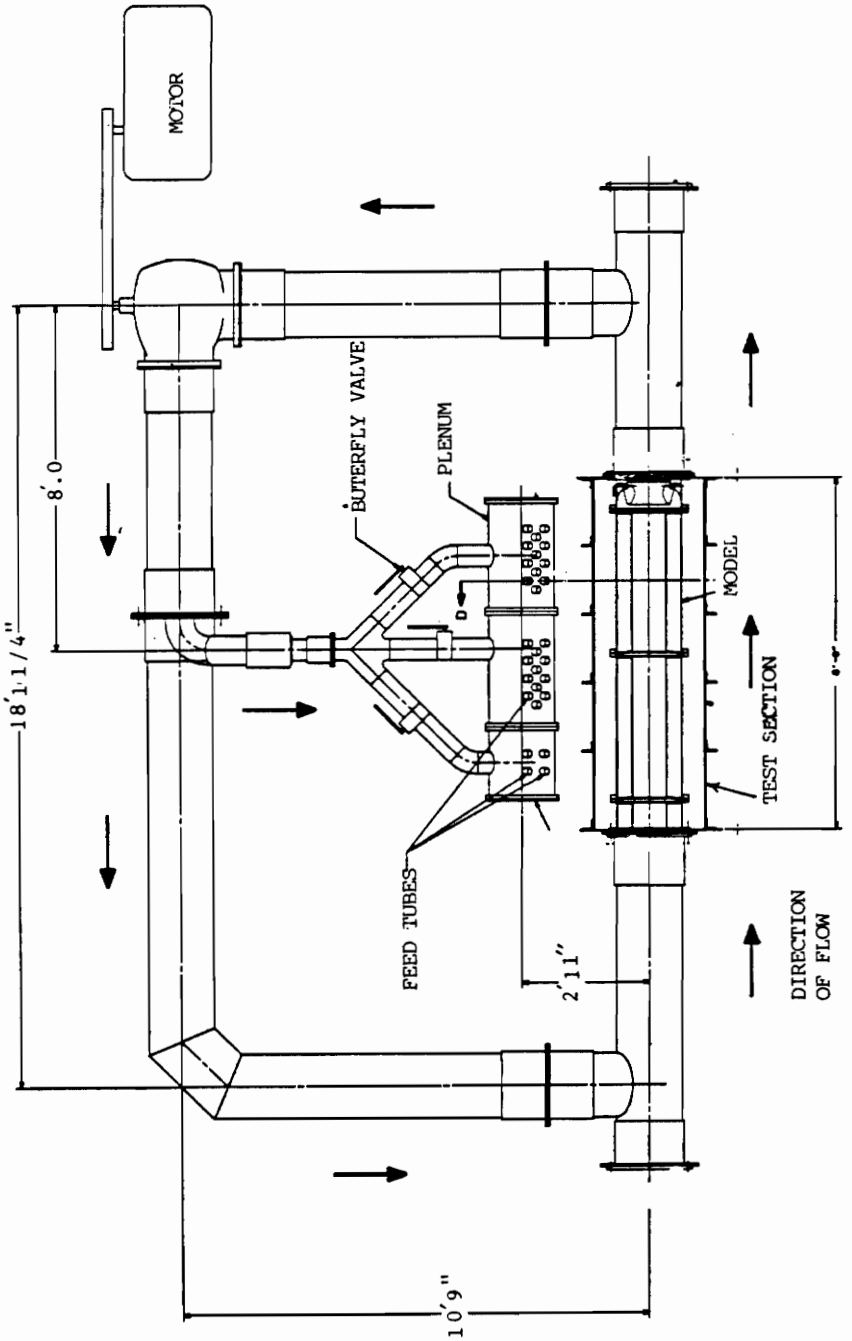

FIGURE 5 DRAWING OF WATER TUNNEL WITH MODEL

each and were connected to the second and third sections of the model respectively. Each model section simulated one full scale booster segment.

Just before the three 5 1/4 inch pipes connect to the plenum section, static and total pressure tubes were mounted to determine flow rates. Velocity profiles were recorded for each of these pipes. In the main tunnel, velocity profiles were recorded by a March McBirney electromagnetic current meter mounted just upstream of the test section. The data from the first 5 1/4 inch pipe and the upstream section of the main tunnel was linear and therefore readings taken from the middle of the pipe sections were used to determine flow rates. The second and third 5 1/4 inch pipes both had uniform curved velocity profiles such that readings taken at the center of each pipe also provided an accurate average reading of flow rates.

The water was circulated by a 7 horsepower motor that could pump approximately 600 gallons per minute. Water tunnel sections were comprised of 18 inch PVC pipe supported by a metal and wood frame. The water speed through the model ranged from 4 to 16 inches per second. A honeycomb seal was located just upstream of the test section. and was designed to eliminate swirl in the flow caused by

water turning at the corners. It also acted to eliminate some turbulence. More detail on the actual water tunnel facility is contained in reference <8>.

Prior to performing the experiment, it was necessary to eliminate air from the water because air bubbles would stick to the model sides and prevent good visibility. Several methods were tried including heating the water prior to water tunnel filling. The method that worked the best was the use of photoflow solution commonly used in film processing. Small amounts of photoflow (about 1 ounce per 500 gallons) was added to the water tunnel. The tunnel was run for 10-15 minutes prior to the experiment to allow for a thorough mixing.

3.0 MODEL DETAILS

A one eighth scale SRM model was constructed of transparent plexiglas. This sizing was chosen primarily because the commercial availability of plexiglas piping was limited to 18 inches in diameter. As mentioned before the SRM model was comprised of a nozzle, two propellant sections and 20 percent of a third booster segment. (The actual SRM contains four booster segments.) Figure (6) shows the model schematic. The model was designed and constructed to enable simulation

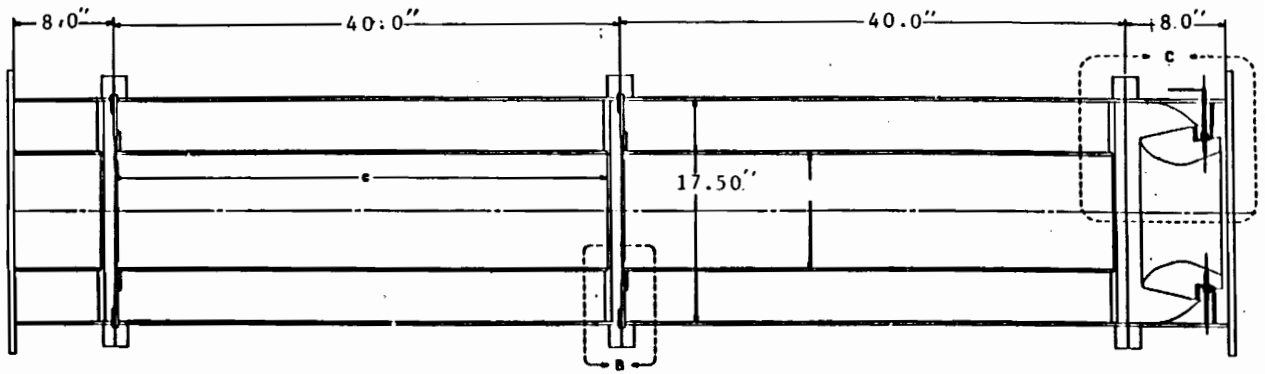

VIEW A
SCALE, NONE

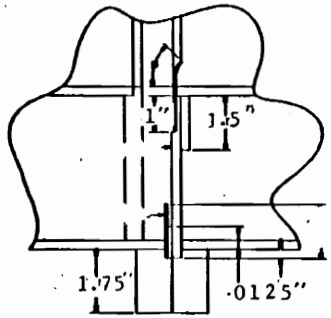

VIEW B
SCALE 1/1

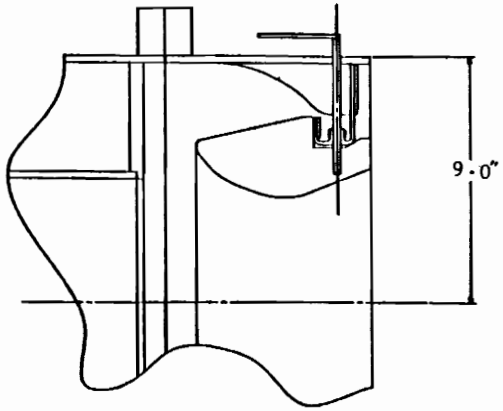

VIEW C
SCALE 2/3

FIGURE 6 DRAWING OF TEST MODEL

of rocket burns at 10, 60 and 100 seconds. This was accomplished by using various size plexiglas pipe inserts mounted inside the main 18 inch pipe. An 8 inch insert pipe was used for the 10 second case, 13 inches for the 60 second case and no insert for the 100 second case. Each of the inserts contained approximately one thousand holes. Water pumped into the sides of the model flowed through these holes simulating the burning propellant. These inserts were supported inside the main 18 inch pipe by flanges at the front and rear. The rear flange also contained holes to allow passage of water flow to simulate burning propellant. The front flange did not contain any holes and modeled the top of the propellant covered by an inhibitor.

The four sections of 18 inch pipe (3 SRM segments and the nozzle) were joined together by 1 inch thick circular rings glued to the outside of the 18 inch pipe. These rings were bolted together in ten places. In the joint between the two booster sections, two spacers were installed. The thicker of the two spacers modeled the connecting flange region. The smaller spacer modeled part of the inhibitor. Figure (4) shows the joint at 10 and 60 seconds.

Water from the plenum was pumped through polyurethane tubes connected to the model by sections of PVC pipe

whcih were capped at the ends. The capped ends contained slits to provide a wide flow dispersion circumferentially along the model casing. In this way the side flow's radial momentum was destroyed and disruptive effects on the core stream were prevented. Also, the exits of the PVC pipes were sized to match the cross sectional area of the polyurethane tubes. Thus, pressure drops were minimized and cavitation was prevented.

Sections of plexiglas were stacked to form a rough shape of the nozzle and then glued together. Afterwards, the nozzle was milled to proper dimensions. The nozzle was mounted on a pivot to allow for swiveling during testing. Figure (7) shows a sketch of the model in the water tunnel with the connecting polyurethane tubing.

4.0 FLOW BALANCING

Flow balancing is the procedure by which the water flow through the main section of the water tunnel and the side flow are set to simulate the SRM. The objective of flow balancing was to match the ratio of core stream and side flow to the actual SRM. In other words, mass flow rate through the side of each segment divided by the mass flow through that section should be equal to the actual SRM. Since there are four main sections on the actual SRM, each

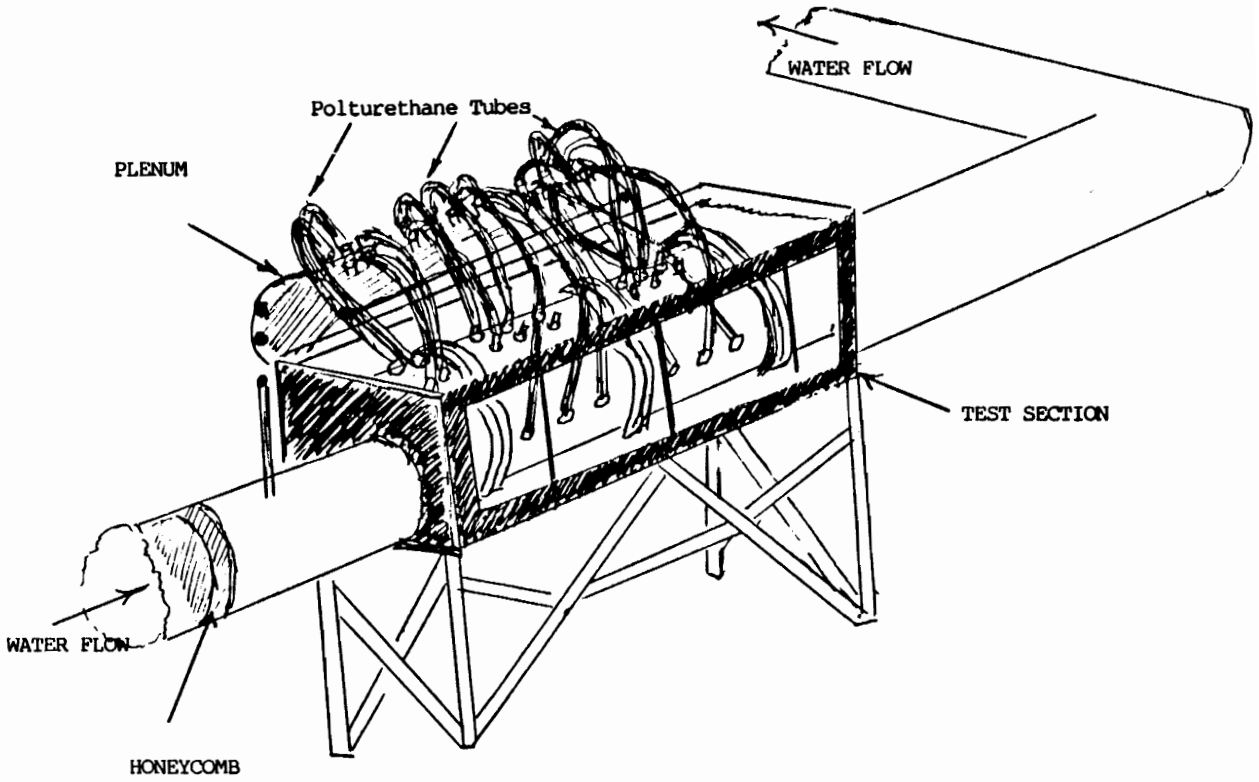

FIGURE 7

SKETCH OF WATER TUNNEL WITH MODEL

model SRM segment should contribute 25 percent of the flow. Therefore, 25 percent of the water tunnel flow is diverted from the main tunnel through the second plenum sections and into the second segment of the booster model. Twenty five percent of the flow is also diverted for the third model segment. Because the upstream segment models 20 percent of a booster segment, only 5 percent of the flow is diverted to this segment. However, this approximation is only good for the 10 second case. Since the propellant burns back, the overall volume ratio of this section is less for the 60 second case and therefore only 4 percent side flow is required to maintain proper simulation.

The actual balancing was accomplished after purging all air in the tunnel and the tubing connecting the model and plenum sections. As mentioned before, water manometers were used to determine mass flow rates in the plenum sections and an electromagnetic current meter for the same purpose in the main section. Because of the relatively small flow rates, it was necessary to mount the manometers on an angle. For each of the manometers, the difference in static and total pressure water heights was read and then corrected for static conditions. Velocities and flow rates were then calculated. Flow rate requirements for the 10 and 60 second burn cases were established for different total tunnel flow rates. Total flow was determined by adding all four flow rates.

Table (I) shows the flow rates used in this investigation and their respective manometer settings for the 10 and 60 second cases. The butterfly valves were adjusted to provide the approximate flow. The manometers were then read and each valve precisely adjusted until the correct manometer reading was obtained. This procedure was repeated several times since adjusting the flow in one valve changes the flow in the others.

For the 60 second case mass flow through the downstream plenum (section 3) was set for maximum flow rate. The resulting flow was slightly less than desired. However, subsequent investigations of varying flow rates indicated that small variations in side flow did not affect any of the observed flow phenomena.

For the 100 second case, only 10 percent of flow could be diverted through all of the sections in the plenum. If more than 10 percent of the flow was diverted, uneven and often circumferential flow would be created inside the model. In the 10 and 60 second cases, the perforated plexiglas inserts prevented circumferential flow from occurring. However, because of the relatively large cross sectional area of the core stream for the 100 second case, it is believed that most of the flow seen by the booster joints and nozzle segment could be adequately modeled by an axial flow. Therefore, no insert tubes were used. This modeling

TABLE I
FLOW RATES AND MANOMETER SETTINGS

10 SECOND CASE TOTAL FLOW RATE: 510 GPM

	% FLOW	FLOW RATE (FT3/SEC)	DELTA H (INCHES)	READ (INCHES)
SECTION 1	5	0.056814	0.026624	0.110055
SECTION 2	25	0.28407	0.665619	1.331238
SECTION 3	25	0.28047	0.665619	1.331238
MAIN SECTION	45	0.511326	0.019609	

60 SECOND CASE TOTAL FLOW RATE: 590 GPM

	% FLOW	FLOW RATE (FT3/SEC)	DELTA H (INCHES)	READ (INCHES)
SECTION 1	4	0.052580	0.022804	0.094265
SECTION 2	25	0.32863	0.890818	1.781637
SECTION 3	23	0.302339	0.753989	1.507978
MAIN SECTION	48	0.617824	0.028628	

technique was deemed adequate, despite the lack of a simulated grain surface.

5.0 EXPERIMENTAL METHODS

Seven methods were used to investigate flow behavior in the nozzle region. Only three of the seven methods tried produced and useable results. The experimental procedures used are described below.

FLUORESCEIN DYE INJECTION

As part of the initial investigation <8>, fluorescein dye was injected into various ports at the top of the model. The resulting flow patterns were recorded by videotape. The dye was injected at points two inches behind and two inches in front of the nozzle just inside the model casing. Dye was also injected just in front of the nozzle at the bottom of the model. This was repeated for 10, 60, and 100 second cases with nozzle at angles between +8 and - 6 degrees (+ is nozzle pivoted up and - is nozzle pivoted down).

BEAD INJECTIONS

Neutral and positive buoyant colored polypropylene beads were injected at various locations in the nozzle

region. Video tapes were made of the flow patterns traced by the beads.

HOT WATER INJECTION

Mr. S. Kuppa provided the necessary setup and computer data acquisition facilities to conduct hot water injection analysis <8>. The objective of this investigation was to determine the circumferential flow rates. Thermocouples were located at specific points in the model to sense minute temperature differentials caused by the hot water injection. The first thermocouple was mounted just inside the casing wall on the top, 2 inches downstream (behind) the nozzle lip. Five more thermocouples were mounted at 30 degree increments around the circumference of the model casing (figure (8)). Hot water was injected next to the first thermocouple and the output of all thermocouples was recorded for twenty seconds utilizing an IBM personal computer with an analog-to-digital board.

The above methods were all done as part of the initial investigation and more detail is provided in reference <8>.

MILK BASED DYE INJECTION

Heavier dye utilizing milk and food coloring was

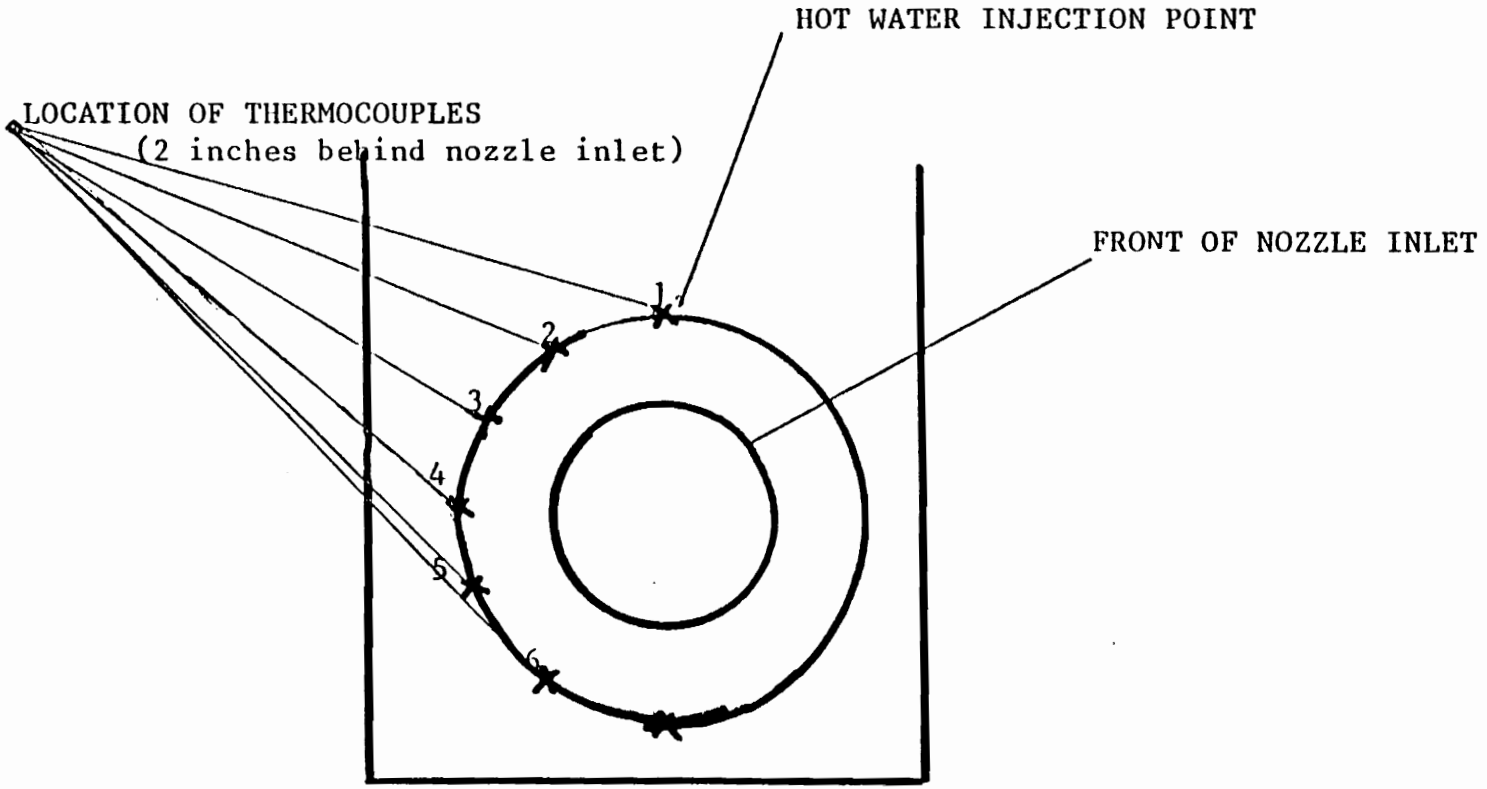

THERMOCOUPLE LOCATIONS
(LOOKING DOWNSTREAM)

Figure 8

injected at the bottom of the model along the wall. It was intended to trap the heavier dye in the boundary layer at the bottom of the model casing so that a vortex could entrain the dye in its core for visualization.

YARN TUFTS FLOW VISUALIZATION

Kite string (in place of yarn) was cut in quarter inch segments and attached to the model wall from zero to 180 degrees. The area approximately two inches in front of the nozzle and two inches behind the nozzle was covered by yarn tufts. Longer segments up to two inches (which extended just short of the nozzle inlet) were also tried. In a final attempt, a wire screen was constructed with quarter inch segments of string attached at half inch intervals. This screen was fitted to the front of the nozzle and secured by duct tape.

HYDROGEN BUBBLE VISUALIZATION

This technique used 0.025 millimeter tungsten wire spread across the flow area. Disassociation of hydrogen gas from the water molecule occurs when wire hooked to the anode of a DC circuit is place in water. The resulting hydrogen bubbles were small enough that they could act as flow pattern tracers

for a short distance when properly illuminated with light. Various wire patterns were used including wire taped to the circumference of the model casing, and various cross field patterns (wire perpendicular to the flow just in front of the nozzle). Sodium sulfate was added to help ionize the water.

VORTEX BUBBLE ENTRAPMENT

This technique evolved from the dye and hydrogen bubble visualization work. During the dye injection investigations, air trapped in the top of the model near the nozzle inlet would periodically get siphoned into the core stream by a vortex and then pass into the nozzle. During the hydrogen bubble investigations, the frequency of the observed vortices increased.

This increase in observed vortices was attributed to the much smaller size of the hydrogen bubbles. During the dye injections, air bubbles present in the model were several times larger than the hydrogen bubbles (which were roughly the same size as the diameter of the tungsten wire). These air bubbles often formed larger pockets of gas at the top of the model. Cohesive forces of the larger gas pockets prevented entrainment of air into the vortex. As a result, fewer vortices were observed. In contrast, the smaller

hydrogen bubbles often stick to the sides of the model rather than collecting at the top in a gas pocket. Therefore, there was less cohesive force to restrict bubble entrainment into the vortex and weaker vortices could be seen. Also, hydrogen bubbles cover a larger area increasing the chance that a vortex could be spotted.

Chromel wires (0.1 millimeter) were placed along the top wall of the model to take advantage of the better vortex detection that hydrogen bubbles provided. These wires covered a region from two inches in front of the nozzle to two inches behind the nozzle from -30 to +30 degrees. The wires were spaced approximately 1/2 inch apart. Zero degrees is considered to be at the 12 O'clock position on the inside of the 18 inch pipe looking downstream. Negative degrees refers to the quadrant marked out between 9 O'Clock and 12 O'Clock. Positive degrees is the quadrant marked out between 12 O Clock and 3 O Clock. A cathode consisting of a sheet of aluminum foil folded into a 3 by 11 inch section was taped to the inside of the nozzle section toward the rear of the aft dome between 6 O'Clock and 3 O'Clock. The chromel wires were fed a small current (1-2 milliamps) with voltages between 40 and 100 volts to generate a continuous source of bubbles. A halogen light was located at the opposite side of the test section from the camera. Video recordings were made

using the negative screen for better contrast of the vortices. Figure (9) shows the test set up. On at least two occasions, wire placed along the wall downstream of the nozzle lip broke. These runs were eliminated from the analysis. It was not always feasible to tear the model down to replace the broken wire since it could take eight or more hours. To save time wire was placed through holes drilled in the model in the vicinity of the broken wire to resupply the model with a source of bubbles. Visual observation indicated that the region of interest did get covered with sufficient bubbles for further vortex observations.

6.0 EXPERIMENTAL RESULTS

As mentioned before, video tape was used to record data. Summary of these written results are highlighted in a separate video tape. For the purpose for this text, results will be described below.

DYE INJECTION

10 Second Case

For the 10 second case, injections were made at an upstream port approximately 6 inches upstream of the nozzle.

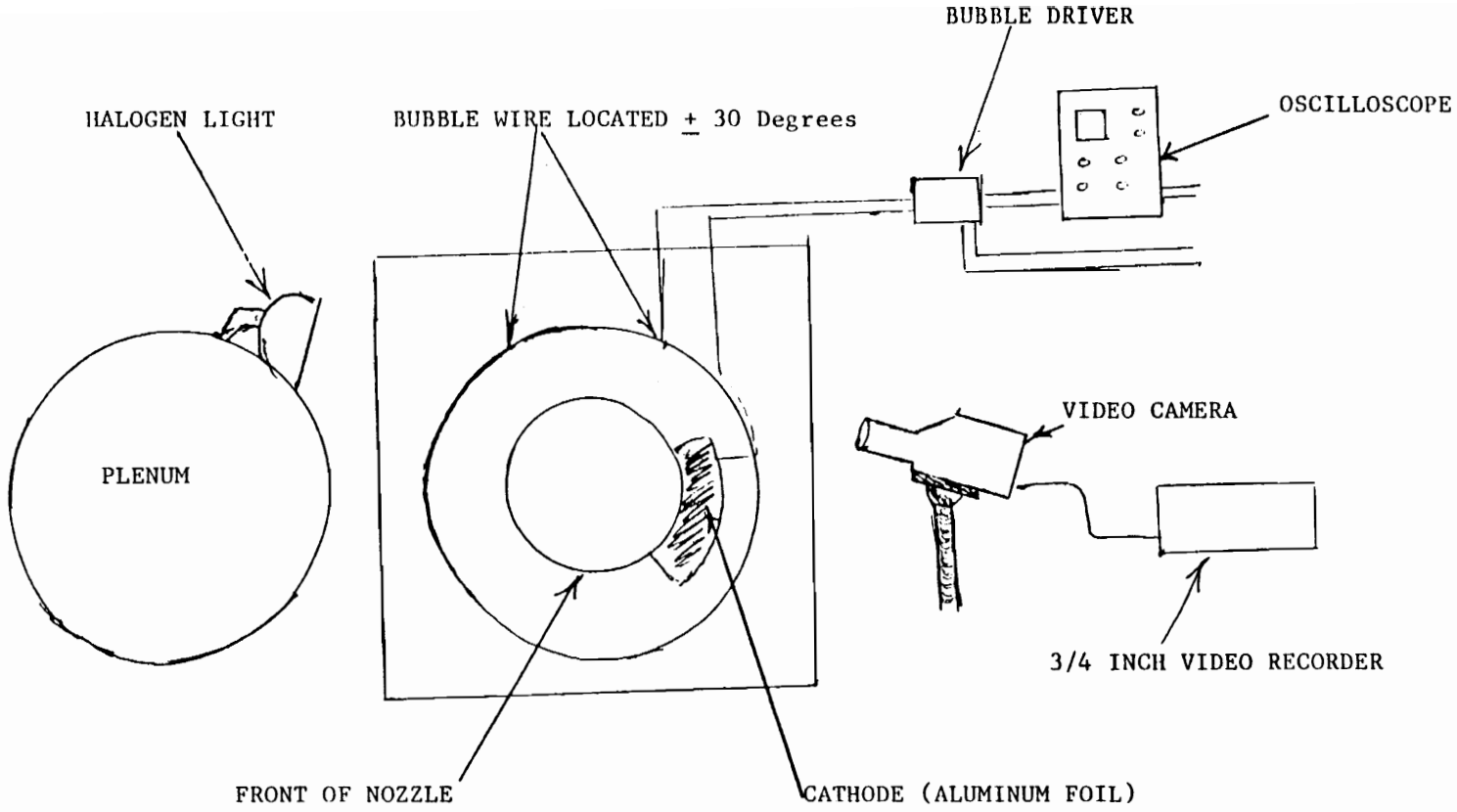

VORTEX BUBBLE ENTRAPMENT TEST SET UP
(LOOKING DOWNSTREAM)

Figure 9

Injections were made across the flow path and most all of the dye was entrained into the nozzle region. Only when injecting between the propellant grain and the outer casing did a small portion get trapped in the nozzle aft dome region for a brief period of time.

Only the extreme pivoted positions (+8 and -6 degrees) produced any noticeable circumferential flow. Dye injected at the top and 2 inches downstream of the nozzle lip when the nozzle was pivoted could be seen to flow circumferentially around the nozzle. Circumferential flow would pass away from the point where the nozzle was farthest from the wall up to the point where it was closest and then turn back on itself. Figure (10) shows the observed circumferential flows.

60 Second Case

For the 60 second case, circumferential flow was found to be the strongest at the extreme pivot angles and was stronger than the 10 second case. Some circumferential flow could be found at $\pm$6 and $\pm$4 degrees positions.

When the nozzle was set at +2 degrees and dye was injected at the top and 2 inches downstream of the nozzle, the dye was observed to remain in the region longer than the +4, +6 or +8 degree cases. In the zero degree case the

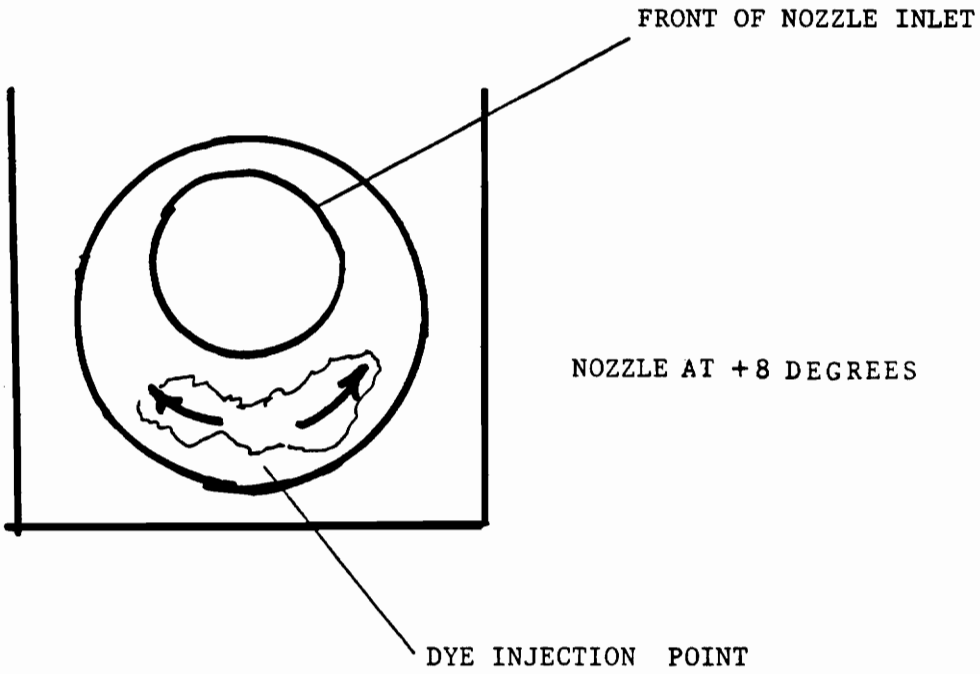
FRONT OF NOZZLE INLET
NOZZLE AT +8 DEGREES
DYE INJECTION POINT
CIRCUMFERENTIAL FLOW OF DYE
(LOOKING DOWNSTREAM)

Figure 10

recirculation region could be seen with no apparent swirl or circumferential flow. Figure (11) shows the recirculation that was seen.

When dye was injected below and downstream of the nozzle (set at +8 degrees), some circumferential flow could be seen. Recirculation flowing upstream was again seen. At +6 degrees the circumferential flow was still apparent and flowed completely around the nozzle. At +4 degrees the circumferential flow still extends to the model top but more slowly.

100 Second Case

For the 100 second case, only 10 percent flow was diverted through the plenum sections. In the third SRM segment, only the four hoses farthest upstream were used. The others hoses in that section were clamped shut. As mentioned earlier, this was done to eliminate flow disturbances induced by side flow. As a control check, the tests were repeated with no bypass flow. In each case, the circumferential and recirculation flows were essentially identical.

Circumferential flow and vortical motion were seen at all pivot positions and were strongest at the extreme pivot angles.

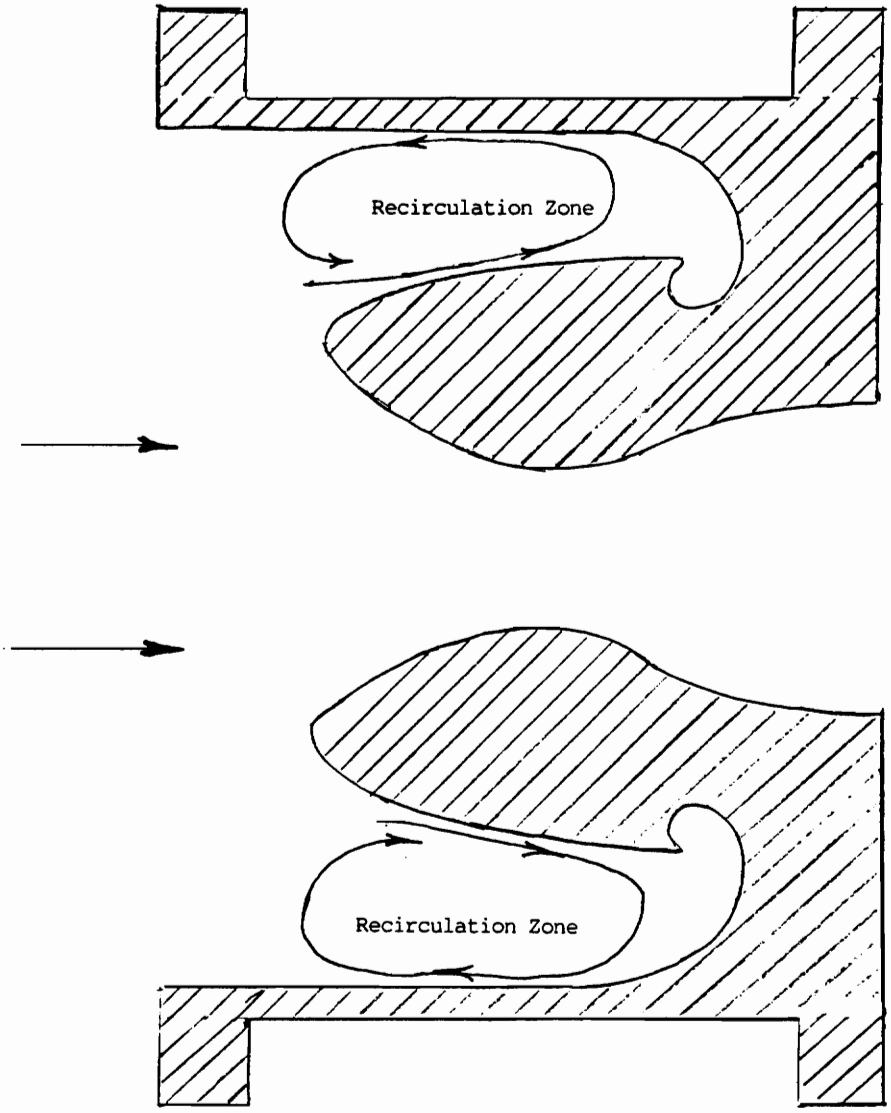

RECIRCULATION FIGURE

Figure 11

Also, the circumferential flow was stronger than the 60 second case. With the nozzle set at +8 degrees and injections made at the top two inches downstream of the nozzle entrance, dye was immediately drawn into the nozzle. Occasionally, some dye would be caught in an apparent vortex and remain in the aft dome for three to four seconds. Circumferential flow to about 4 O'Clock could also be seen. With the nozzle still at +8 degrees and injecting along the casing below the nozzle, circumferential flow going above 3 O'Clock could be seen. Dye was injected 3 inches upstream of the nozzle and approximately 1/2 inch inside the casing. Most of the dye was entrained directly into the nozzle.

With the nozzle at -6 degrees, recirculation flow along the casing wall was also seen. This flow came approximately 3 to 4 inches upstream of the nozzle. With the nozzle at - 6 degrees and injecting dye at the top of the model downstream of the nozzle lip, circumferential flow was observed. With the nozzle set at zero degrees and injections made at the top, 2 inches behind the nozzle lip, some circumferential flow to about 3 O'Clock was seen. Dye was then injected at the bottom and the same pattern was observed. When dye was injected 1 inch inside the model casing and 3 inches upstream of the nozzle,

lip, some dye was caught in a vortex at the top and remained for a brief amount of time. This was not a consistent event. Usually the dye would be rapidly drawn into the nozzle.

BEAD INJECTION

Neutral buoyant beads were injected into the nozzle region. Because of turbulent conditions, no significant results could be detected. Lighter beads injected into the model also failed to produce results. The intent of this method was to allow a tracer (the beads) to get stuck in the boundary layer on the wall and be drawn into a vortex core for visualization. However the beads only stuck to the wall of the model and none were entrained into a vortex core.

HOT WATER INJECTION

A relative temperature (TREL) was determined from the thermocouple measurements. This temperature was computed as follows:

$$T(REL) = \frac{T(I,J) - T(0,J)}{TMAX - T(0,1)}$$

T(I,J) = The temperature of the Jth thermocouple at the Ith time.

T(0,J) = The initial temperature of the Jth thermocouple

TMAX = The maximum temperature recorded at all the thermocouples during a particular run

T(0,1) = The initial temperature of the first thermocouple

In all cases only the first three thermocouples produced any significant results. Often these thermocouples would show spikes in the data. Some of the more interesting graphs are presented in figures (12) through (16). (Complete sets of graphs are included in reference <8>.) The spikes on some of the graphs are fairly consistent, with the time period between the spikes lasting between 2 and 3 seconds. It is believed that these results indicate the hot water caught in a recirculation region between the nozzle and the model wall. On many of the figures, no particular trend could be identified. This is believed to be a result of the turbulent and vortical conditions.

MILK BASED DYE INJECTION

This technique produced no results. Flow turbulence quickly diluted the dye in the water and made any meaningful results impossible.

YARN TUFT VISUALIZATION

This technique was not successful. Again the reason

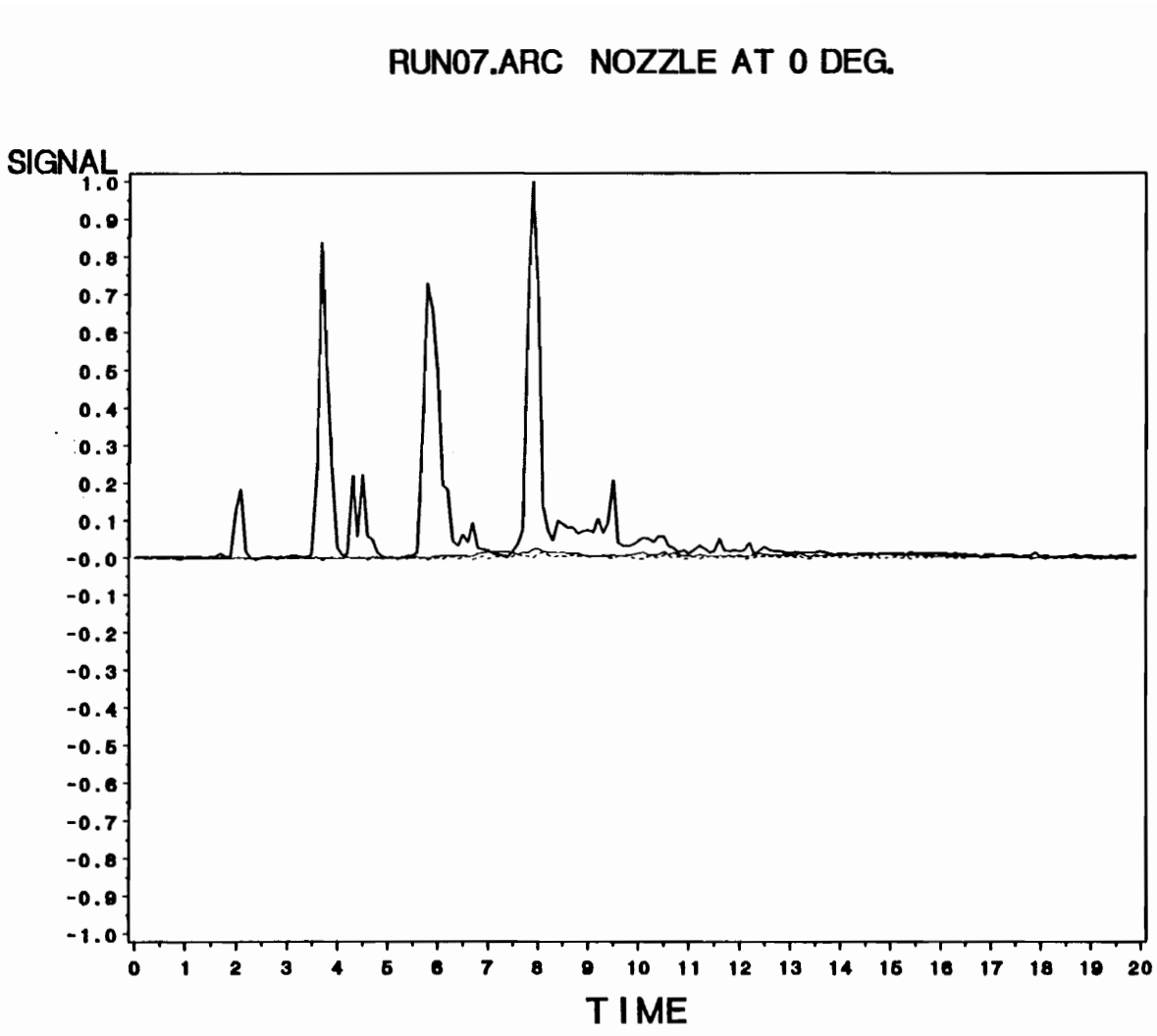
RUN07.ARC NOZZLE AT 0 DEG.
SIGNAL
1.0
0.9
0.8
0.7
0.6
0.5
0.4
0.3
0.2
0.1
-0.0
-0.1
-0.2
-0.3
-0.4
-0.5
-0.6
-0.7
-0.8
-0.9
-1.0
0 1 2 3 4 5 6 7 8 9 10 11 12 13 14 15 16 17 18 19 20
TIME
THC.CHANNEL#1------DARK SOLID LINE
THC.CHANNEL#2------GREY SOLID LINE
THC.CHANNEL#3------DASHED LINE

FIGURE 12

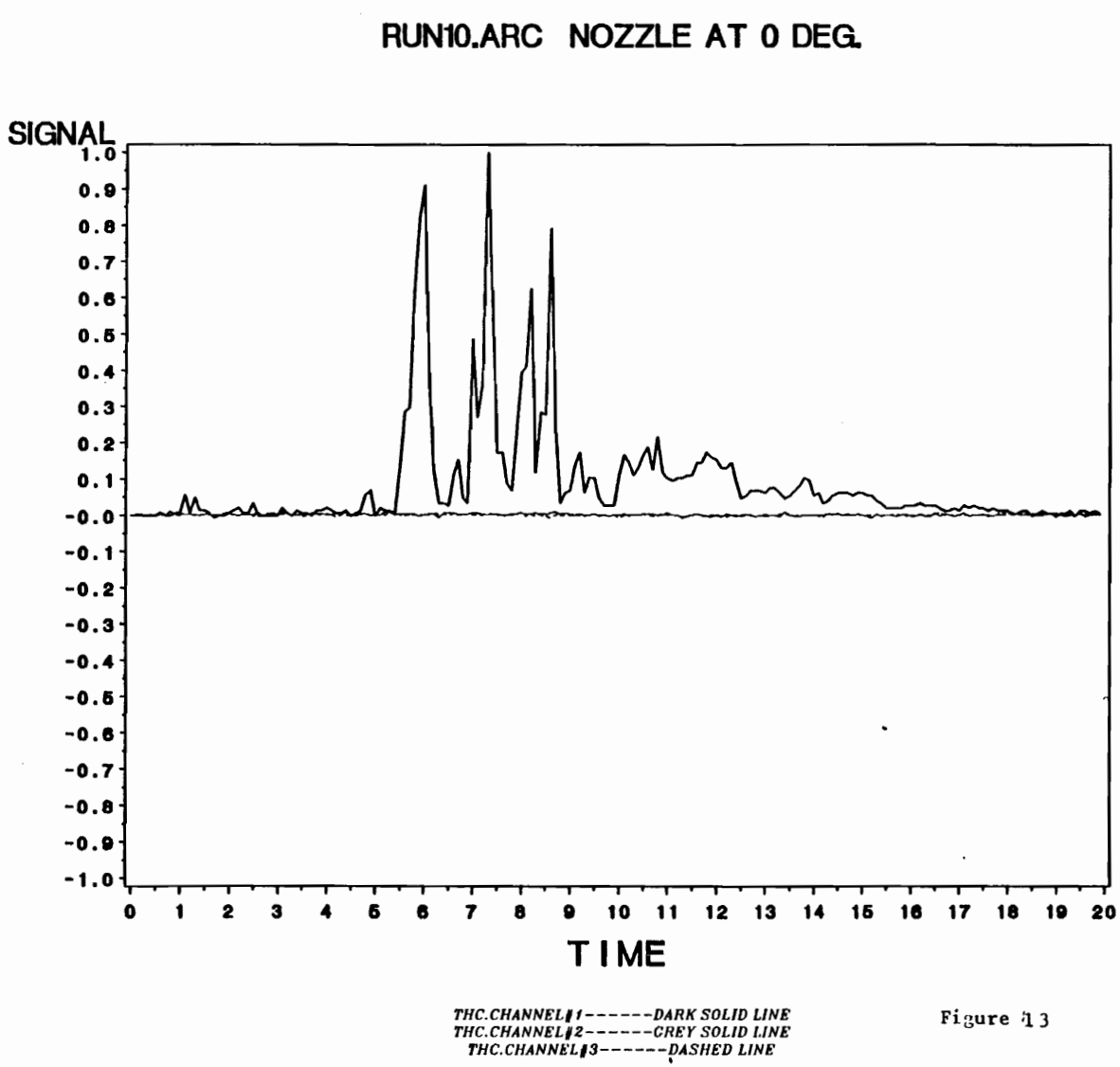
RUN10.ARC NOZZLE AT 0 DEG.
SIGNAL
1.0
0.9
0.8
0.7
0.6
0.5
0.4
0.3
0.2
0.1
-0.0
-0.1
-0.2
-0.3
-0.4
-0.5
-0.6
-0.7
-0.8
-0.9
-1.0
0 1 2 3 4 5 6 7 8 9 10 11 12 13 14 15 16 17 18 19 20
TIME
THC.CHANNEL#1------DARK SOLID LINE
THC.CHANNEL#2------GREY SOLID LINE
THC.CHANNEL#3------DASHED LINE

Figure 13

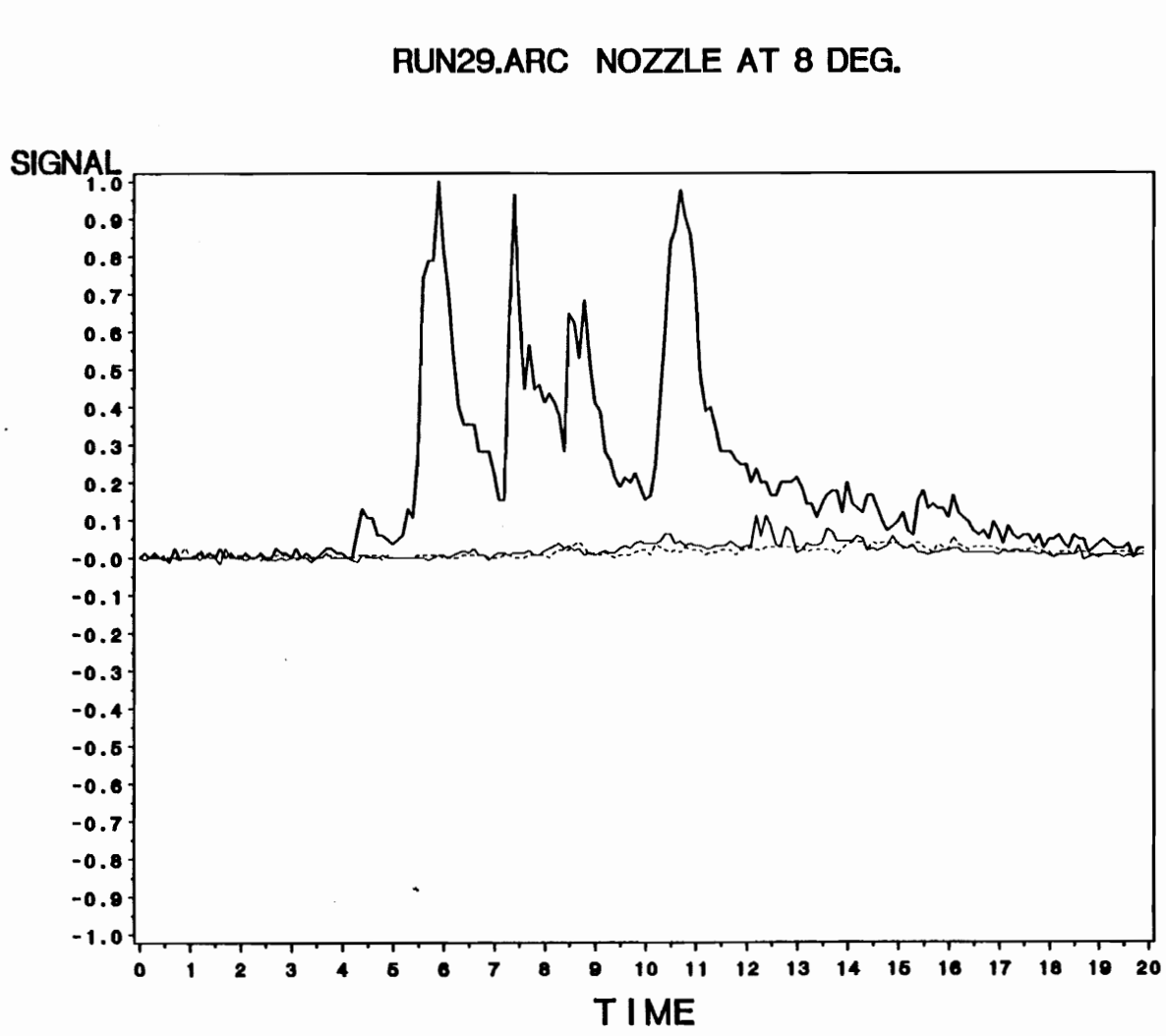
RUN29.ARC NOZZLE AT 8 DEG.
SIGNAL
1.0
0.9
0.8
0.7
0.6
0.5
0.4
0.3
0.2
0.1
-0.0
-0.1
-0.2
-0.3
-0.4
-0.5
-0.6
-0.7
-0.8
-0.9
-1.0
0 1 2 3 4 5 6 7 8 9 10 11 12 13 14 15 16 17 18 19 20
TIME
THC.CHANNEL#1------DARK SOLID LINE
THC.CHANNEL#2------GREY SOLID LINE
THC.CHANNEL#3------DASHED LINE

FIGURE 14

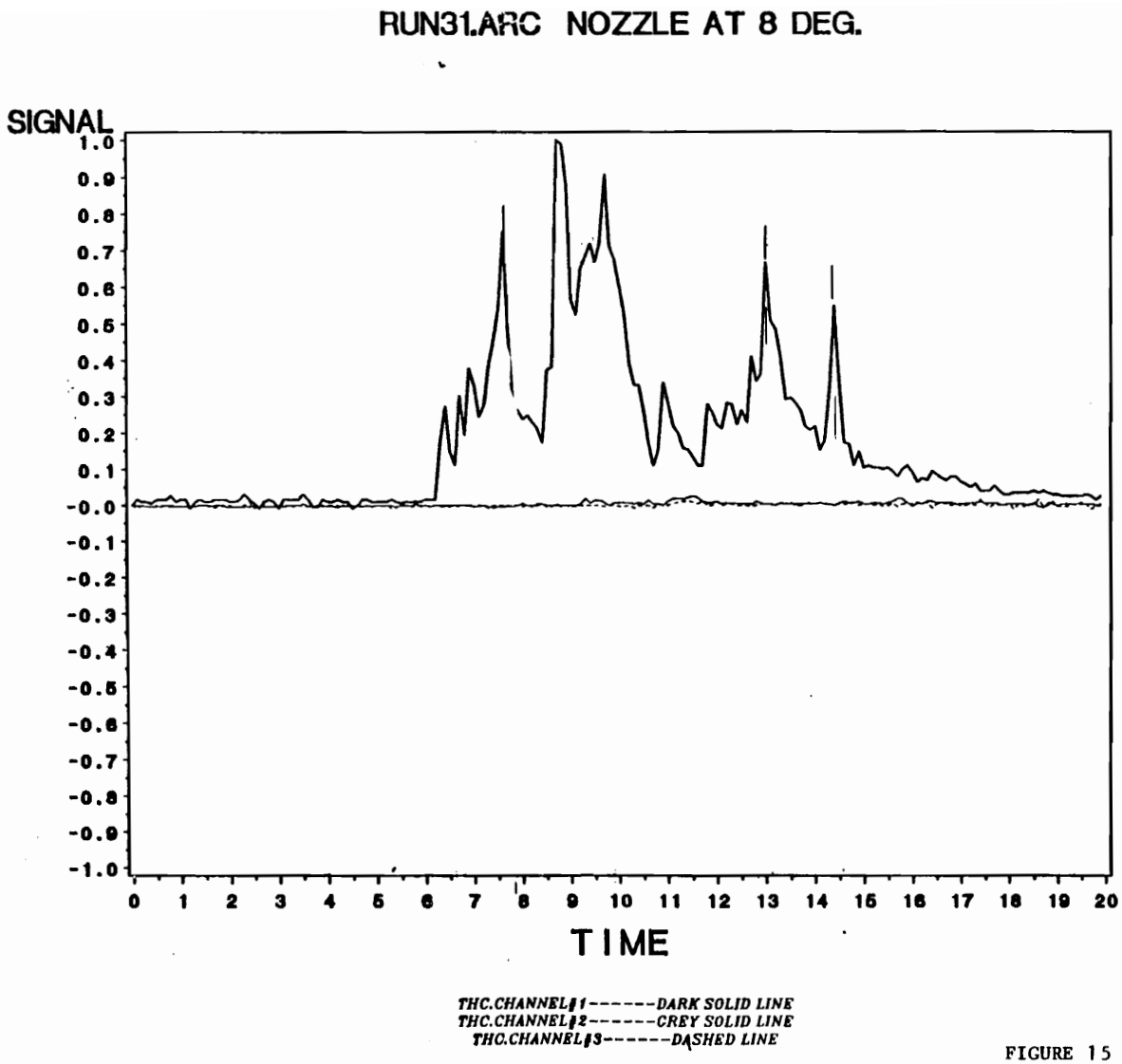
RUN31.ARC NOZZLE AT 8 DEG.
SIGNAL
1.0
0.9
0.8
0.7
0.6
0.5
0.4
0.3
0.2
0.1
-0.0
-0.1
-0.2
-0.3
-0.4
-0.5
-0.6
-0.7
-0.8
-0.9
-1.0
0 1 2 3 4 5 6 7 8 9 10 11 12 13 14 15 16 17 18 19 20
TIME
THC.CHANNEL#1------DARK SOLID LINE
THC.CHANNEL#2------GREY SOLID LINE
THC.CHANNEL#3------DASHED LINE

FIGURE 15

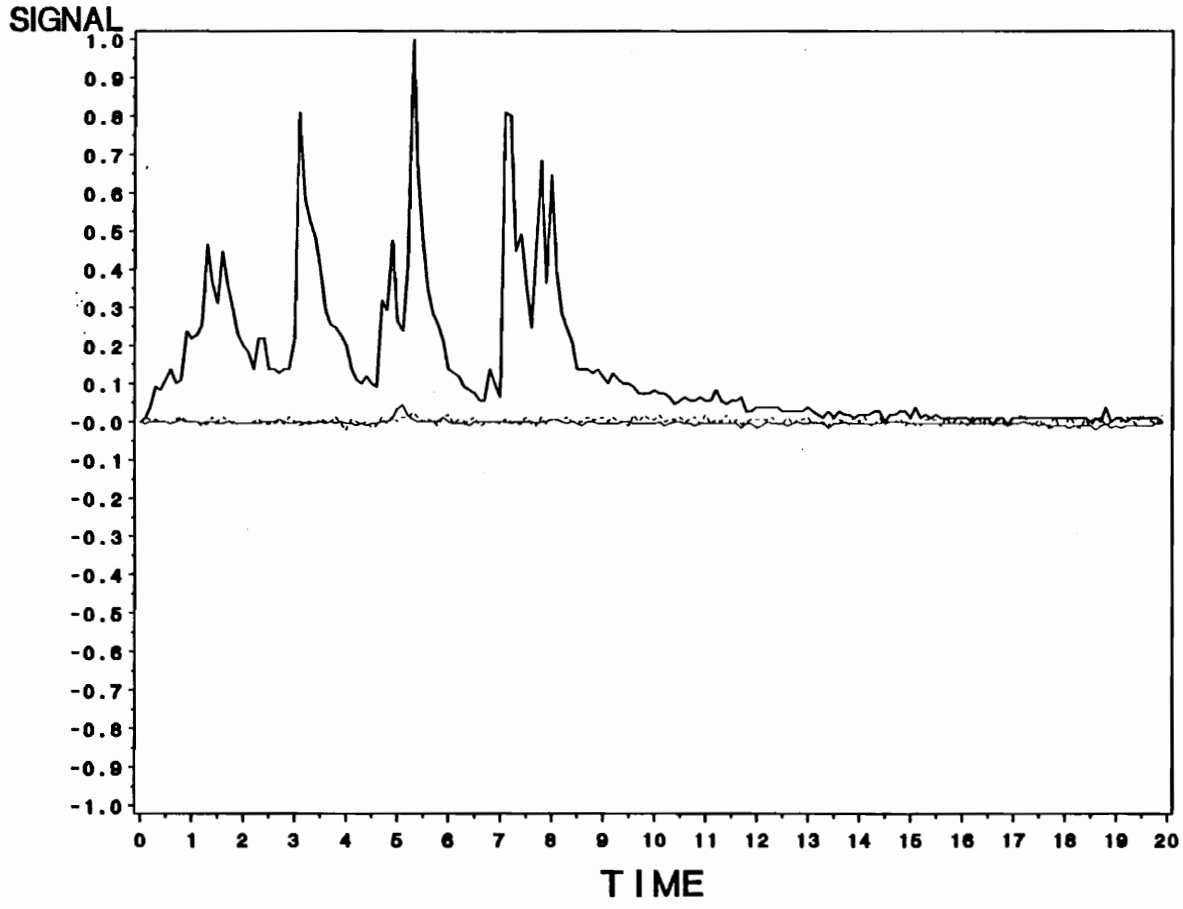

THC.CHANNEL#1------DARK SOLID LINE
THC.CHANNEL#2------GREY SOLID LINE
THC.CHANNEL#3------DASHED LINE

FIGURE 16

believed for lack of results was the extreme turbulent mixing that created many flow disturbances that hindered vortex visualization.

HYDROGEN BUBBLE GENERATION

This technique also failed to produce significant results, because of turbulent mixing. In addition this technique is very dependent on proper light placement. The area of interest was located at the rear of the tunnel. The steel plate which makes up the rear of the tunnel and the close proximity of the plenum section prevented proper light placement. The overall size of the model was also too large for good bubble visualization because too much wire was required to cover the flow path. The longer wire required greater current and voltages than the facilities could provide. In other water tunnel work <18,19>, the size of the model used was much smaller and hence, the amount of wire used was less. Therefore, smaller currents and voltages were required to produce enough bubbles for good visualization.

VORTEX BUBBLE ENTRAPMENT

This technique was the most successful for providing visual and quantitative results of vortex behavior. The zero degree case was chosen because results gathered in

one sector could be assumed constant around the nozzle circumference due to symmetry. Only the top section where the bubbles collected could be studied at any one time. The 60 second case was chosen to study because it provided the best conditions for vortex observation. Few vortices were evident during the 10 second case and the 100 second case was not considered because modeling propellant grain was very difficult.

Seven runs twenty minutes long were done and all results recorded on video tapes. The video tapes were replayed and time and location of vortices were noted. The region which vortices occurred was between 5 and 10 degrees on either side of the 12´Oclock position and from two inches upstream to three inches downstream of the nozzle lip. Because the nozzle flanges obstructed the view, it was not possible to clearly identify what point the vortices occurred between 0 and +10 (this is the area between the 12:00 and 12:30 looking downstream at the nozzle).

Vortices of different strengths and durations were observed. Vortex duration was usually about a second but some would last as long as 4 to 5 seconds. Some vortices would begin to form and die out before reaching the nozzle. Other vortices formed in the aft dome area between the nozzle outside wall and the model wall. Also, observed were inlet trailing vortices (these are not to be confused with

aircraft wing trailing vortices). Their core lies along the nozzle surface and extends to the rear of the aft dome. Figure (17) shows the various vortices observed. Because of the varying duration and strengths of vortices, it is believed that some vortices would be strong enough to propagate a disturbance throughout the core flow. Based on this assumption, observed vortices were classified as either significant or insignificant. A significant vortex is defined as any vortex which entrains gas into the nozzle. Vortices which did not entrain air into the nozzle were considered insignificant vortices. Insignificant vortices were believed to be either too weak or too far removed from the main stream to affect the core stream and hence produce a disturbance which could propagate.

Figure (18) shows all the vortices and times when they formed. Figure (19) shows the vortex formation rates. Formation rates were timed from the occurrence of the first significant vortex to the formation of the next significant vortex (i.e., if a significant vortex was observed to occur at Time A and the next significant vortex forms at Time B, the difference between Time A and B is identified as the vortex formation rate). Although a varying vortex formation rate was observed, a time of approximately four minutes and 15

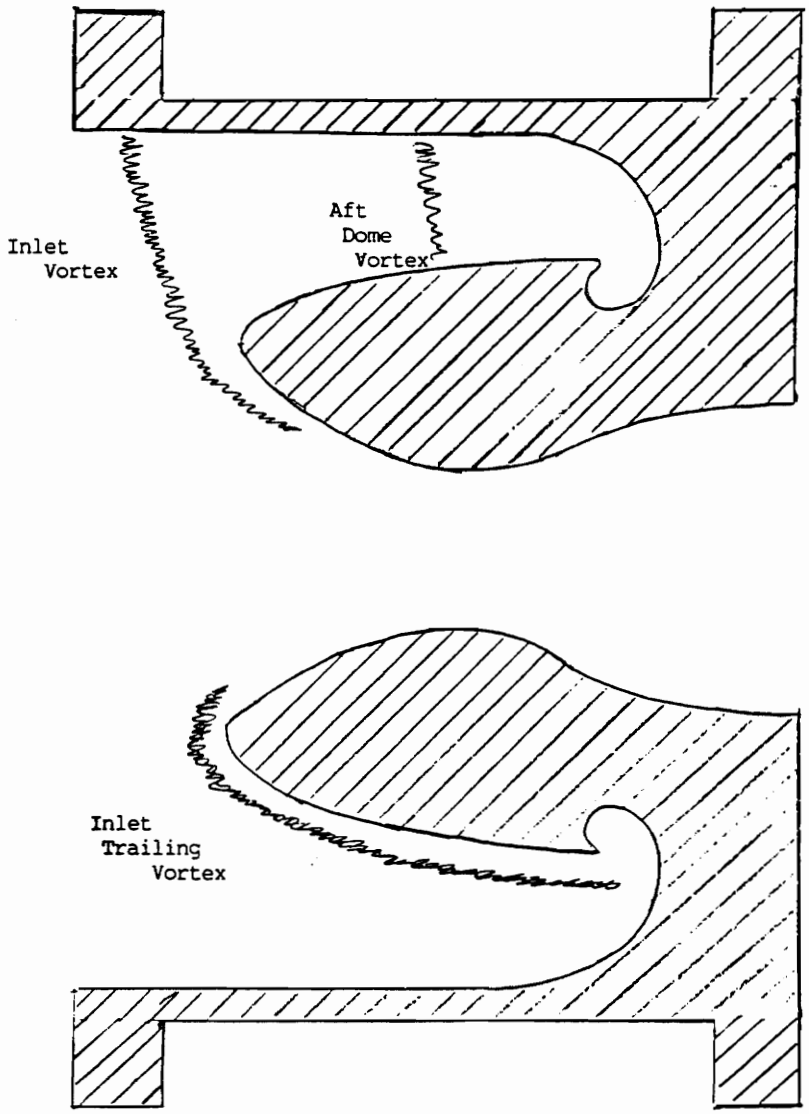

OBSERVED VORTICES

Figure 17

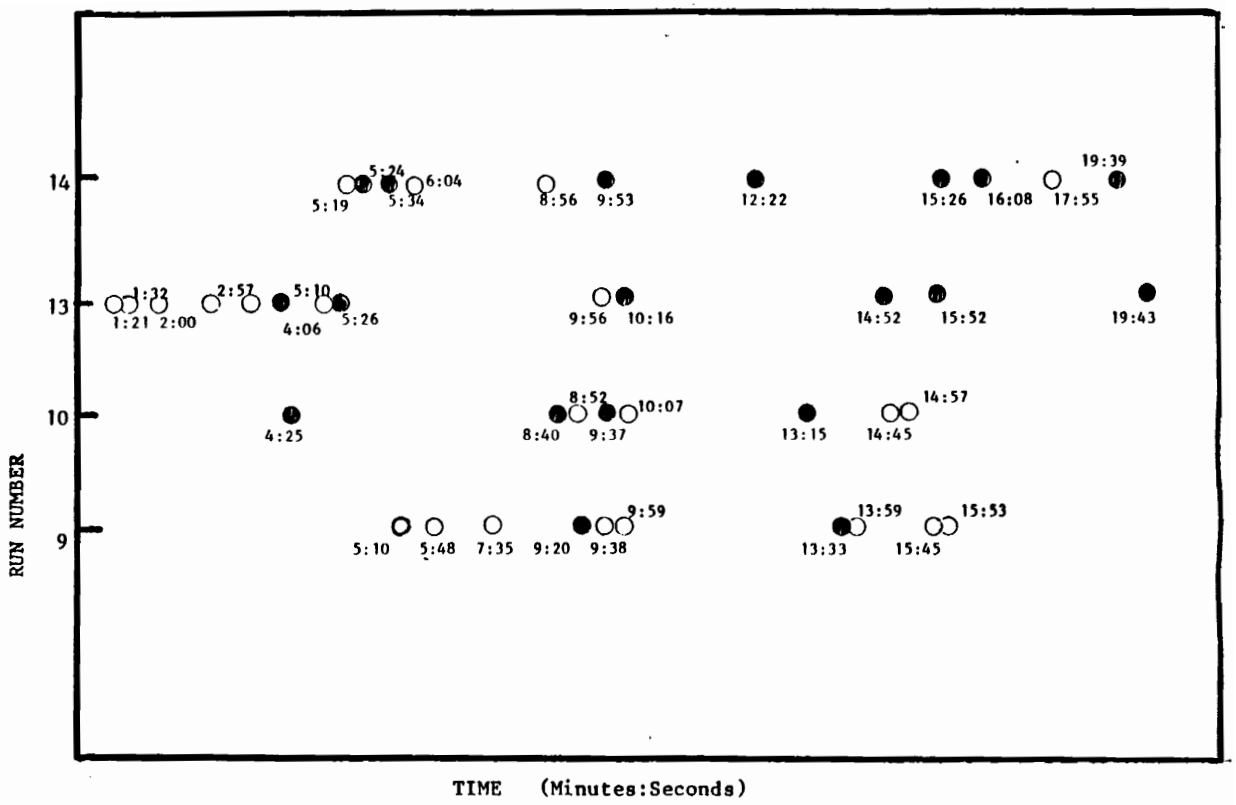

FIGURE 18 VORTEX FORMATION TIMES

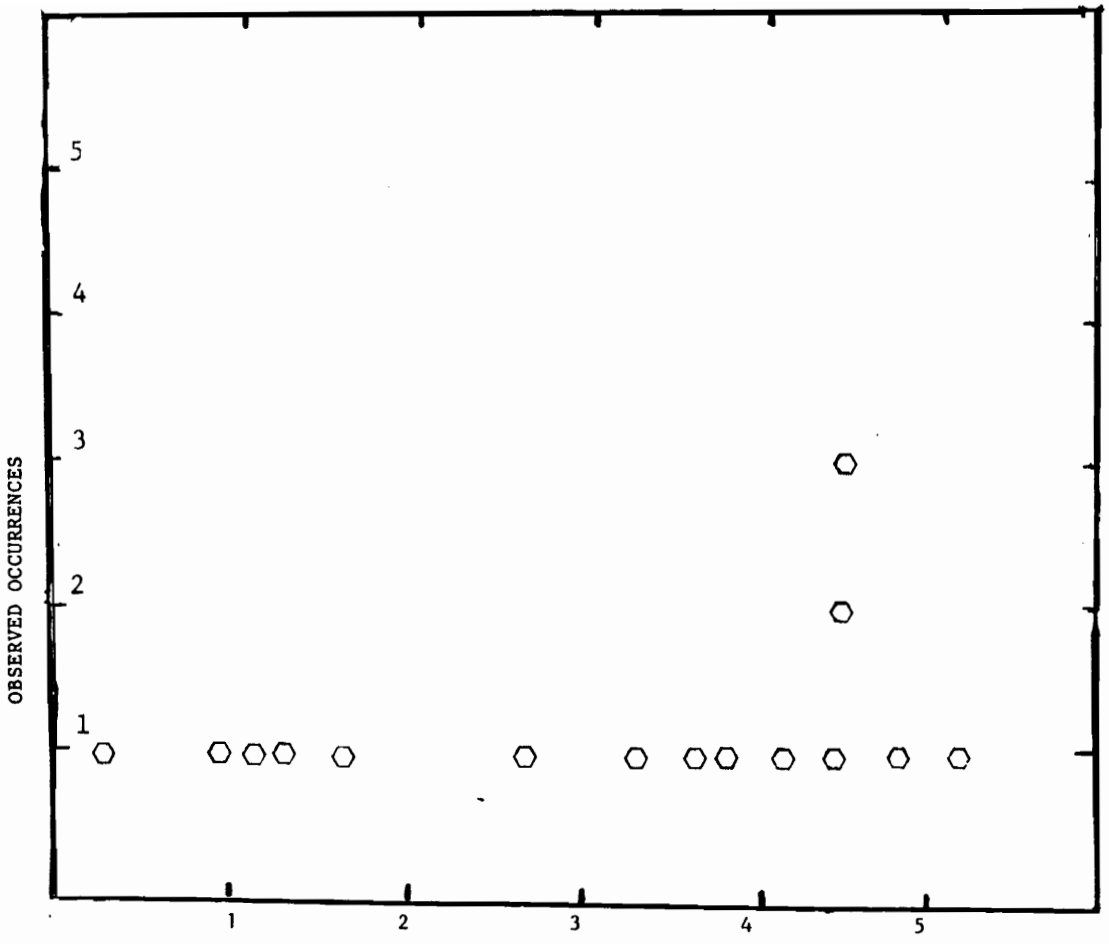

FIGURE 19 VORTEX FORMATION RATES

Note: A formation rate was recorded to occur more than once if another vortex had a formation time within 5 secs

seconds (+ or - 5 seconds) was observed in 3 cases. This seemed to be unusual number of times for this rate to occur considering the small amount of data taken. Also much of the data seemed to be centered around this time.

7.0 DISCUSSION

Three different types of flow phenomena were observed during these investigations. They included circumferential, recirculatory and vortical.

The results analyzed were primarily from the 60 second case because they provided the best case for studying the circumferential and vortical flow patterns.

The circumferential flow patterns were primarily a function of pivot angle and were observed in the 60 and 100 second cases. Other analyses done for Morton Thiokol and presented at the Circumferential Flow Conference <1-4> indicated a fair amount of agreement of the circumferential flow patterns in the nozzle section. Many types of analysis were used including advanced computational fluid dynamics.

Circumferential flows were determined from the dye injection video tapes to be on the order of 3 to 4 inches per second for the 8 degree case and 2 1/2 to 3 1/2 inches per second for the 6 degree case. For the 100 second case the

velocity was found to be as high as 8 inches per second for the 8 degree case and about 4 to 5 inches per second for the 6 degree case. Velocities were determined by measuring the time it took for dye to travel from a point 180 degrees from where the nozzle was closest to the wall and the approximated point on the nozzle circumference where the dye enters the nozzle. (There were no marked points on the circumference. The stopping point was determined by approximating it with reference to a clock, i.e., 10:00, 10:30.) Because of the slower velocities for the smaller angles ($\pm$4 to 0 degrees) reliable measurements could not be made.

It is believed that the hot water data (from the thermocouple measurements) provided substantiation of the recirculation areas seen during the dye injections. The time in between temperature spikes was fairly consistent (approximately 2 to 3 seconds). This would correlate to a recirculation velocity of about 5 to 7 inches per second, or which is about 33 to 45 percent of the core stream velocity. The core stream velocity was measured on the center line just outside the nozzle inlet. In the many cases in which there was no evidence of any particular periodicity, it is believed that either a vortex or the turbulent conditions prevented detection of circumferential or recirculation flows.

During the 60 second case, many vortices were observed.

These vortices were believed to be caused by side flow which simulated the burning propellant. The vortices seen in this experiment closely resembled vortices seen in front of engine inlets operating close to the ground. It was reasoned that the casing in the SRM acts like the ground does for engine inlets. Therefore, many of the analyses and studies done for engine inlet vortices were believed to be applicable to the SRM investigation.

In work done by MIT <18>, an engine inlet was modeled and several methods tried to induce vortices. It was concluded that vortex creation was caused by upstream vorticity collecting at the stagnation streamline in front of the inlet. As the vortex core becomes ingested into the nozzle, it is stretched, thereby shrinking the vortex core diameter. Since the strength of a vortex core remains constant along its axis, the speed of the rotating core must increase and therefore a drop in pressure occurs creating the vortex. Bissinger's work <19> with hydrogen bubble visualization and engine inlets also confirmed the requirement that upstream vorticity and a stagnation point located near the inlet is required for vortex formation. The recirculation zone creates a natural stagnation point close to the nozzle inlet.

Also, the vortices were believed to be influenced by the additive effects of the recirculation occurring in the aft dome region and the vortex line stretching effects caused by the nozzle. It is believed the recirculation accentuates the nozzle effects by stretching the vortex line farther downstream along the outside of the nozzle. The recirculation effects were believed to be evident in the investigation by several vortices seen which only appeared between the model case and the outside nozzle wall in the aft dome area. Other vortices were also seen which started in front of the nozzle and were blown back into the aft dome area.

As mentioned previously, water tunnel work has shown good agreement with actual combustion systems. Other studies of vortical flows in water tunnels have also shown good agreement with actual vortical behavior in air. In the work done by McDaniels at University Institute of Tennessee <20>, relevant water tunnel work was reviewed with the emphasis of determining the accuracy of using a water tunnel to model flow phenomena that occurred in air. McDaniel's surveyed the work done by Erickson <21> who modeled vortices formed on delta wings in a water tunnel. A close correlation could be made between vortex trajectories observed from actual delta

wings and those modeled in a water tunnel. However, secondary vortices which formed as a result of boundary layer conditions could not be modeled accurately. The main conclusion drawn from this investigation was that vortices formed from other than boundary conditions could be modeled accurately in a water tunnel with very little dependence on Reynolds number.

It is believed that the vortices observed in this experiment resulted from upstream side flow injection and was not a boundary layer condition. Therefore, the work by Erickson and McDaniels is thought to provide some substantiation that the vortices seen in the SRM investigation may be an accurate representation of the actual SRM. The assumption that side flow injection causes the vorticity seems to be reasonable because there certainly would be some type of velocity profile induced in the flow. This flow combined with the viscosity of the fluid could cause vorticity. Other possible causes of vorticity may be vortex rings originating from the inhibitors. The resulting vortex lines are then stretched by the nozzle to form vortices. In this investigation, vortex rings from the inhibitors were not believed to occur. The flow around the inhibitors was examined and no evidence of ring vortices could be found. Side water injection was believed to destroy any type of vortical flow from the inhibitors.

In the work done by Klein <22>, engine inlets were modeled using a vacuum cleaner. The results of his work produced threshold limits by which a particle can be predicted to be ingested into an inlet. Klein used two parameters. One was engine inlet to ground height ratio and inlet velocity to free stream velocity. Klein did his correlation between a model with a Reynolds number of 7.97×10^4 and full scale inlet which had a Reynolds number of 6.71×10^7. Klein work's was repeated and confirmed by Colehur and Farquear <23>.

Also Bissinger's work found that the same two parameters were the most significant to determine vortex type and structure. The ratio to model inlet height to ground (model casing) is equivalent to the actual SRM casing. If core stream velocity is equated to the free stream velocity, then Bissinger's second parameter (free stream to engine inlet velocity) is also equivalent for the model and the actual SRM. Therefore the vortex structure and strength should correlate with the actual SRM.

Additionally, if the rate of side flow is accepted to be the cause of the vorticity, then the amount of vorticity created should be equal for the model and SRM because the ratio of model side flow to core stream is equal to the actual SRM.

It can be shown that the vortex formation rate of 4 minutes 15 seconds is close to the actual SRM 15 Hz observed pressure oscillations. This can be shown as follows:

The model nozzle inlet velocity was measured to be;

(measured by dye movement on the nozzle center line)

Model Nozzle Core Flow = 15.3 in/sec = VM

Now the actual inlet core flow on the SRM has been computed to be;

Actual Nozzle Core Flow = 18,669 in/sec =VA

Since the model is 1/8th scale, a time scaling can be established as follows:

$$\frac{T(Model)}{T(Actual)} = 1/8 \times VA/VM$$

Substituting in the velocities,

T(Model) = 152.5 X T(Actual)

The approximate region which vortices were observed was about 15 degrees (from 11:30 to 12:30) which assuming the same vortex formation rate around the circumference corresponds to a vortex formation rate of about,

255 SecM/24 = 1 vortex forming approximately every 10.625 seconds This equates to the full scale SRM vortex formation rate of:

10.625 secM =(10.625 secM X 1 secA/152.5 secM)

T(Actual) = 0.0697 Secs = 14.35 HZ

This formation rate correlates very closely with actual 1-L pressure oscillation frequency detected on full scale SRM test firings. The validity of the four minute 15 second vortex formation rate can be argued because it was based on a small amount of data and the author's interpretation of what was a significant and insignificant vortex. However, there is a trend present in the observed vortex formation times (figure (18)). Every three to four minutes a series of vortices form. This appears to be too consistent to be considered a coincident.

In the actual SRM test firings, vibration is not detected until about the 40 second point. Also, in this investigation strong vortices were not seen until the 60 second case. The smaller diameter bore with the early burn cases may prevent vortex formation because there is insufficient room to allow a vortex line to be stretched prior to ingestion into the nozzle. Also until the grain burns back, the recirculation region may not be fully developed and therefore a stagnation point may not be present.

It should be noted that during the actual shuttle launches (and test SRM firings), the nozzle operates on a duty

cycle which involves pivoting to about 4 degrees. As was seen in the extreme pivoted cases (+ or - 8 degrees), the vortex location and strength are altered. Whether or not the pivoting of the nozzle has any effect on significant vortex formation rates is not known.

The second potential problem vortices may pose is the disruptive force caused by the low pressure core. The breakage of wire on the wall during the hydrogen bubble and vortex bubble entrapment runs was believed to be a reflection of this problem. Vortex action is responsible for damage to aircraft engines <19,22,23>. Aircraft inlets operated close to the ground ingest foreign objects which often damage the engine. The larger size and higher internal SRM velocities could cause much stronger vortices. These vortices could potentially affect insulation or other parts of the nozzle section that may have been weakened by other means (burning, etc.). Also, their potential for creating a disturbance which could propagate throughout the rocket is likely to be greater.

During the end of this investigation, some inlet trailing vortices were observed. Bissinger saw similar types of vortices. These vortices were not observed regularly through this investigation because no hydrogen bubble wires were located in the rear of the aft dome area.

These vortices were believed to be visible as a result of a continual build up of oxygen bubbles on the cathode. The cathode was located at the rear of the aft dome and just below where vortices were observed to originate.

Most of the modeling techniques used and read about during the course of this investigation were based on Reynolds numbers. Other methods that use different non-dimensional parameters could have possibly been used.

8.0 CONCLUSIONS

This experiment provided very useful insight into various flow patterns that are believed to occur in the nozzle region of the SRM. Previous studies have shown that water tunnel work can be used to accurately model hot combustion chambers and vortex behavior. For the 60 second case circumferential flows as high as 25 percent of the nozzle core flow were observed at the extreme nozzle pivot angles. Recirculation is predicted to be as high as 45 percent of the nozzle core stream flow. Both the circumferential flow patterns and the recirculation flows can contribute to increased convective heating which has obvious detrimental effects to the casing and insulation.

The vortices observed are also of particular concern

because they cause disturbances which may propagate throughout the rocket. The test data indicated that vortices may occur at the frequency necessary to induce SRM acoustic pressure oscillations.

9.0 RECOMMENDATIONS FOR FUTURE WORK

Considerable effort was spent trying to develop a technique to visualize and count vortices. Although the bubble entrapment method is a crude technique, there are some lessons learned that could improve results.

Close attention should be paid to the water condition. Photoflow used to increase visibility, adversely affected the hydrogen bubble's ability to stick to the model walls. The result was a smaller area of bubble coverage and increased size of bubbles collecting at the top of the model. Thus, fewer vortices could be spotted. For this type of flow study, none or very little photoflow is recommended. Other techniques such as heating the water before filling the water tunnel may be useful in eliminating problems caused by air sticking to the sides of the model.

Also, proper wire selection is important in generating the hydrogen bubbles. Wire that was taped to the sides of the model wall would often break, especially in the area

downstream of the nozzle. In further studies the strongest wire possible should be chosen to provide required bubble size.

The location of the wires should be expanded to cover more of the aft dome area such that vortices in all areas of the nozzle region may be visualized.

It is recommended that the effects of nozzle pivoting be examined to determine their effect on vortex formation rates. The model used in this investigation could be used to determine these rates. This task would require rotating the entire nozzle section with respect to the rest of the model. At the downstream end, the nozzle fits snugly into the tunnel's 18 inch PVC pipe with no attachments and therefore can rotate. Clamps on the flanges could be used to secure the nozzle to the upstream end of the model. By rotating the model in increments, and taking data at each relocation, a composite record of vortex behavior can be compiled.

Also, it is recommended that a grain closer to that of the actual SRM be used. In this investigation the grain was parallel to the casing wall. In the actual SRM the grain burns back faster at the rear of a propellant section. As a result, the grain is tapered in relation to the casing wall.

If the hydrogen bubble wire experiments are to be repeated, a smaller model might be used requiring less wire to cover the flow area. This will allow for better

visualization by producing more visible bubbles.

For the most accurate vortex information, pressure sensors spread across the anticipated vortex formation area could be used for detailed study of vortex behavior.

10.0 References

1. Malone, M. B., "Circumferential Flow Near the SRM Joint" Circumferential Flow Conference Held 28-29 Sept 1987 at Morton Thiokol, Minutes and record of briefings of:

2. Sicilian, J. M., Hirt, C. W., Flow Science, Inc, "Circumferential Flow at Nozzle Joint", Circumferential Flow Conference Held 28-29 Sept 1987 at Morton Thiokol, Minutes and record of briefings of:

3. Prozan, R. J., Sulyman, P. R.,Continum, "Three Dimensional SRM Aft Port Flow Analysis", Circumferential Flow Conference Held 28-29 Sept 1987 at Morton Thiokol, Minutes and record of briefings of:

4. Whitesides, R. H., Ghosh A., Jenkins S. L., SRS "3-D Aft Motor Case Subscale Cold Flow Tests", Circumferential Flow Conference Held 28-29 Sept 1987 at Morton Thiokol, Minutes and record of briefings of:

5. Nguyen, P. M., Morton Thiokol, "CFD Analyses Using the Phoenics Program", Circumferential Flow Conference Held 28-29 Sept 1987 at Morton Thiokol, Minutes and record of briefings of:

6. Sicilian, J. M., Hirt, C. W., Flow Science, Inc. "Influence of Asymmetric Inhibitor at the Aft Joint", Circumferential Flow Conference Held 28-29 Sept 1987 at Morton Thiokol, Minutes and record of briefings of:

7. Taylor, D. D., Hercules, Inc. "CFD Analysis using the Comet Program" Circumferential Flow Conference Held 28-29 Sept 1987 at Morton Thiokol, Minutes and record of briefings of:

8. Marchman, J. F., Neu, W. L., Walker, D. A., Squire, D. E. Qian, X., Kuppa, S., Water Tunnel Tests of the Space Shuttle Solid Rocket Motor Internal Flow, Virginia Tech Aerospace and Ocean Engineering, July 1987

9. Hussey, B., "Acoustic Waveforms in Statically Tested Space Shuttle SRMs", Morton Thiokol Inc. Wasetch Operations

10. Shu P. H., Sforzini R. H., and Foster W.A., Vortex Shedding from Solid Rocket Propellant Inhibitors, Auburn University, under NASA contract NAS8-36147

11. Kennedy, J.B., "Ramburner Flow Visualization Studies," 11th JANNAF Combustion Conference, CPIA Publ. No. 261 pp. 45-440, September 1974.

12. Schetz, J. A., Hewitt, P.A. and Thomas, R., "Swirl Combustor Flow Visualization Studies in a Water Tunnel, " Journal of Spacecraft and Rockets, Vol. 20, No 6, pp 574-582, November-December 1983.

13. Schetz, J.A. Guruswamy, J. and Marchman III, J.F., "Effects of an S Inlet on th Flow in a Dump Combustor," Journal of Spacecraft and Rockets, Vol. 22, No. 2, pp. 221-224, March-April 1985.

14. Schetz, J.A. Sebba, F. and Thomas, R.H., "Flow Visualization Studies of a Solid Fuel Ramjet Combustor Using a New Material Polyaphrons,"22nd JANNAF Combustion Meeting, October 7-11, 1985.

15. Winter, E.F., "Flow Visualization Techniques Applied to Combustion Problems, "Journal of the Royal Aeronautical Society, Vol. 62, pp. 268-276, April 1958

16. Winter, E. F.,Poulston, B. V., "Techniques for the Study if Air flow and Fuel Droplet Distribution in Combustion Systems,"Sixth Symposium (International) on Combustion, Reinhold Publishing Company, New York, pp 833-842, 1956.

17. Winter, E.F. and Deterding, J.H., "Apparatus and Techniques for the Application of a Water Flow System to the Study of Aerodynamic Systems," British Journal of Applied Physics, Vol. 7, No. 7, pp 247-260, July 1956.

18. Viguier, H. C., Greitzer E. M., Tan C. S., Mechanisms of Inlet-Vortex formation, De Siervi, Massachusetts Institute of Technology published in Journal Fluid Mechanics 1982 vol. 124 pp 173-207

19. Bissinger, N. C., On the Inlet Vortex System, P.H.D. Thesis Tennessee University, 1974 74-17,719 (University Microfilms)

20. McDaniels, D., Background and Theoretical Considerations For Utilizing Water Tunnel Flow Visualization, Aug 1986 M.S. thesis UTSI 86-07

21. Erickson, G. E. "Water Tunnel Flow Visualization" Insight into complex three dimensional Flow fields, Journal of Aircraft, Vol 17 No. 9 September 1979

22. Klein H. "Small Scale Tests on Jet Engine Pebble Aspiration," Douglas Aircraft Company Report SM-14885, August 1953

23. Colehur J. L., Farquear B.W., Inlet Vortex Gas, Journal of Aircraft vol 8, 1971

SRM FLOW STUDY TEAM

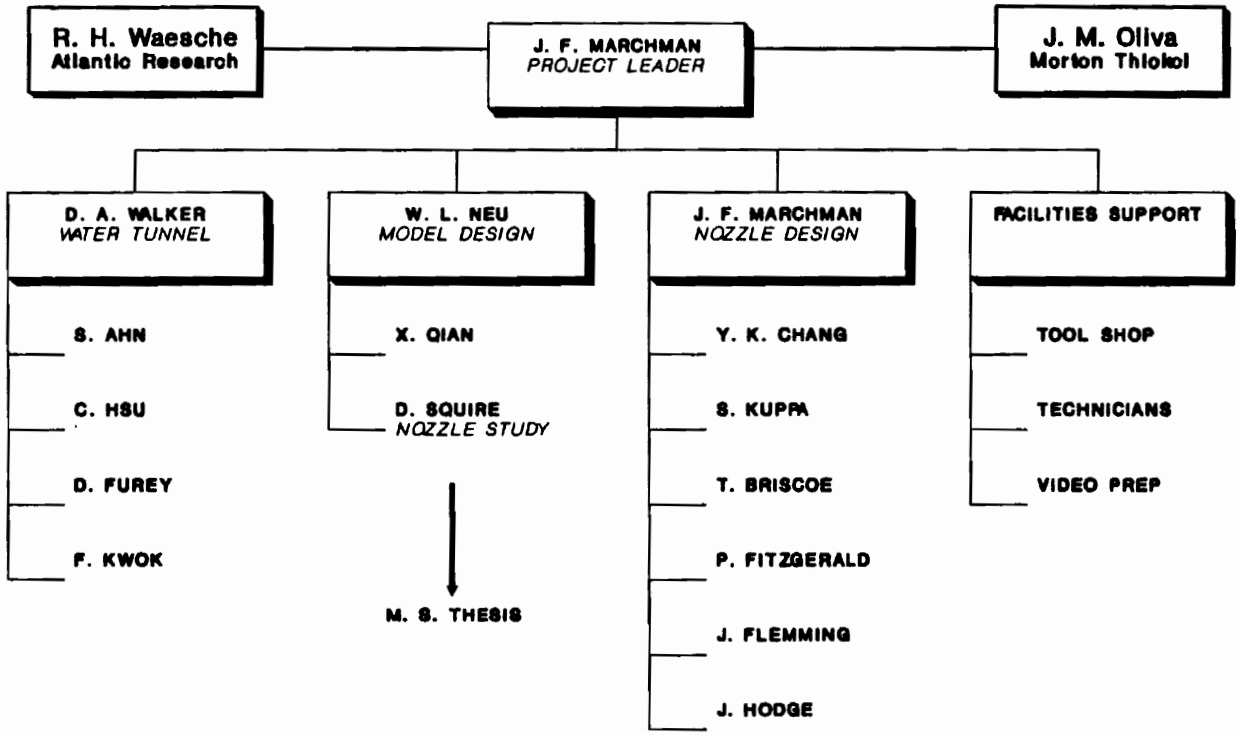

Appendix A.1